1989

Study of photolytic interference on HO measurements by LIF-FAGE

Carmen Ivette Martinez
Portland State University

Recommended Citation
Martinez, Carmen Ivette, "Study of photolytic interference on HO measurements by LIF-FAGE" (1989). *Dissertations and Theses.* Paper 3931.
https://doi.org/10.15760/etd.5815

AN ABSTRACT OF THE THESIS OF Carmen Ivette Martinez for the Master of Science in Chemistry presented November 3, 1989.

Title: Study of Photolytic Interference on HO measurements by LIF-FAGE.

APPROVED BY THE MEMBERS OF THE THESIS COMMITTEE:

[redacted]

Robert J. O'Brien, Chairman

[redacted]

David Peyton

[redacted]

Thomas M. Hard

[redacted]

Jean Murray

For many years there has been a great interest among the scientific community in the study of the hydroxyl radical, HO. This interest stems from the fundamental role played by this molecule in the photochemistry of the atmosphere, mainly as a cleansing agent of environmental pollutants. Knowing the concentration of the radical would enable scientists to corroborate current

atmospheric models and to predict future trends in the atmosphere. Even though there is a great interest in the determination of atmospheric concentrations of this molecule, the task has been very difficult. This is mainly due to the lack of a method sensitive enough to detect concentrations around 10^6 molecules per cubic centimeter. The most accurate method presently available is the method of laser induced fluorescence using the fluorescence assay with gas expansion technique (LIF-FAGE). This method involves low pressure excitation of HO from its ground state to its lowest electronic excited state and observing the consequent fluorescence around 309 nm. The procedure is done at a pressure of 5 Torr to maximize the fluorescence lifetime of the radical and to minimize the interference of photolytic species. Background determination is achieved by chemical modulation using isobutane in a second channel of the same cell which removes the HO signal.

In this study an assessment of the level of ozone interference in LIF-FAGE has been done by calculating the relative population distribution of HO among its rotational levels and from this, determining its temperature. When the laser passes through the excitation detection cell it photolyses the ozone present producing in this way the highly reactive $O^1(D)$. When this molecule reacts with water or with isobutane it produces HO, and this is the source of interference in the actual measurements.

In the determination of the relative population distributions of the different HO species, it was found that the naturally occurring HO has a

thermal distribution with a temperature of about 300 K. The HO molecules produced from the reaction of $O^1(D)$ with isobutane also showed a thermal distribution with a temperature of about 230 K. On the other hand, the HO produced from the reaction of $O^1(D)$ with water did not show a thermal distribution. Two distinct temperatures were observed for this case: one around 200 K for values of K= 1 to 4, and the second one around 3000 K for values of K = 5 to 6. These values agree with previous experimental results for LIF methods by other authors except for the fact that the deviation from the first temperature determined by other authors starts at K = 6 or 7.

STUDY OF PHOTOLYTIC INTERFERENCE ON HO MEASUREMENTS BY LIF-FAGE

by

CARMEN IVETTE MARTINEZ

A thesis submitted in partial fulfillment of the
requirements for the degree of

MASTER OF SCIENCE
in
CHEMISTRY

Portland State University

1989

TO THE OFFICE OF GRADUATE STUDIES:

The members of the Committee approve the thesis of Carmen Ivette Martinez presented November 3, 1989.

[redacted]

Robert J. O'Brien, Chairman

[redacted]

David Peyton

[redacted]

Thomas M. Hard

[redacted]

Jean Murray

APPROVED:

[redacted]

Bruce Brown, Chair, Department of Chemistry

[redacted]

C. William Savery, Vice Provost for Graduate Studies and Research

DEDICATION

To my daughter, Nicole Natassja,

my inspiration and reason for it all.

ACKNOWLEDGEMENTS

I would like to express my gratitude to my advisor, Dr. Robert J. O'Brien for his support throughout the duration of this project and to Dr. Tom M. Hard for his constant guidance and encouragement. Special thanks to Cornelius Chan who worked side by side with me and help me make this project come true.

I would also like to express my gratitude to my parents, to my sister Mercy and to Vahid. Without their love, patience and support this work would have not been possible.

TABLE OF CONTENTS

LIST OF TABLES

LIST OF FIGURES

CHAPTER I

INTRODUCTION

IMPORTANCE OF HYDROXYL RADICAL

For many years the importance of hydroxyl radical, HO, has been recognized in the scientific world. There are two major reasons for the interest in this small molecule. The first one is the understanding of this molecule's physical properties for kinetic and spectroscopical interests. The study of this molecule's energy transfer processes in the excited state would help in the understanding of the kinetics of other excited small molecules. In spectroscopy the interest is to develop model Hamiltonians that could accurately represent the experimental rotational-vibrational states of the molecule.

The second reason for the interest in the study of this molecule is its crucial role in the chemistry of the atmosphere. The importance of hydroxyl radical was first indicated by Bates and Witherspoon (1952) who proposed reactions involving HO and HO_2 as likely sinks for carbon monoxide, CO, and methane, CH_4. However, its dominant role in the tropospheric chemistry of many hydrocarbons and other reactive species was not recognized until Levy (1971) identified the principal sources of HO and predicted appreciable

concentrations in the lower atmosphere. Atmospheric chemists have theorized that ambient HO concentration in the atmosphere is around 10^6 molecules per cm^3. At these low concentrations the very reactive HO radical could be controlling the worldwide conversion of carbon monoxide to carbon dioxide as well as playing an important role in the removal of both naturally occurring trace gases such as methane and anthropogenic ones such as methylchloroform and in this way preventing additional stratospheric ozone destruction.

In 1971 Levy proposed the primary source of HO production to be the photodissociation of ozone at 300 nm producing the metastable singlet oxygen ($O^1(D)$) which in turn reacts with water vapor producing hydroxyl radicals. From this, relatively high concentrations of the radical were calculated for clean air. The hydroxyl radicals could then react with carbon monoxide, ozone and methane to produce hydroperoxyl radicals, which in turn oxidize nitric oxide to nitrogen dioxide and reform hydroxyl radicals (Table I). These chain reactions which rapidly interconvert hydroxyl and hydroperoxyl radicals may provide the dominant mechanism for removing atmospheric carbon monoxide and methane and for producing formaldehyde in the normal atmosphere. The presence of hydroxyl and hydroperoxyl radicals is the basic ingredient for the production of photochemical smog.

Table II gives reactions involving HO, which are very valuable in the understanding of the chemistry of the atmosphere. In assessing the importance

TABLE I

MAJOR PATHS FOR HYDROXYL RADICAL PRODUCTION AND RECYCLING

---

(1) $h\nu + O_3 \rightarrow O^1(D) + O_2$

(2) $O^1(D) + H_2O \rightarrow OH + OH$

(3a) $OH + CO \rightarrow H + CO_2$

(3b) $OH + CH_4 \rightarrow H_2O + CH_3$

(4) $H + O_2 + M \rightarrow HO_2 + M$

(5) $HO_2 + O_3 \rightarrow OH + 2O_2$

(6) $HO_2 + NO \rightarrow OH + NO_2$

(7) $HO_2 + HO_2 \rightarrow H_2O_2 + O_2$

(8) $hv + H_2O_2 \rightarrow OH + OH$

(9) $OH + H_2O_2 \rightarrow H_2O + HO_2$

(10) H_2O_2 + (rain, aerosol) --> products

(11) $OH + NO_2 + M \rightarrow HNO_3 + M$

(12) HNO_3 + (rain,aerosol) --> products

TABLE II

TROPOSPHERIC REACTIONS INVOLVING HO

$OH + CO \rightarrow CO_2 + H$

$OH + CH_4 \rightarrow H_2O + CH_3$

$OH + NO_2 + M \rightarrow HNO_3$

$OH + RH + M \rightarrow H_2O + R$

$OH + CH_xCl_yF_z \rightarrow H_2O + CH_{x-1}Cl_yF_z$

$OH + CH_xBr_y \rightarrow H_2O\ CH_{x-1}Br_y$

of each of these processes relative to other possible competing processes, two major pieces of information are required: (1) absolute rate constants for the elementary reaction of interest and, (2) the concentration of natural tropospheric HO. In the first case nearly all the data is available. However, the second piece of information has been very hard to obtain due to the high sensitivity required in order to detect the predicted low concentrations of 10^5 - 10^7 hydroxyl molecules per cubic centimeter. Many different methods have been used in the attempt to obtain reproducible results. Some of these methods will be discussed in the next section.

DETECTION METHODS

To this date there are six direct and one indirect method for the measurement of hydroxyl radical concentrations. In this section a brief description of each method is given, as well as a consideration of their associated problems. The methods are:

- indirect determination by measurements of atmospheric trace constituents.
- optical absorption (Perner et. al., 1976)
- isotope tracing (Campbell et. al., 1979)
- spin-trapping (Watanabe et. al., 1982)
- laser induced fluorescence at atmospheric pressure in enclosed detection chamber (Davis et. al., 1976, 1979)

- laser induced fluorescence at atmospheric pressure with an open optical arrangement (Wang et. al., 1981)
- laser excited fluorescence using FAGE (Hard et. al., 1984)

Indirect Determination by Measurement of Atmospheric Trace Constituents

Hydroxyl radical concentrations can be determined by the measurement of other tropospheric species if the relationship between these and the hydroxyl radical is known. In 1974 Warneck proposed using the oxidation of NO_2 and the resulting precipitation of nitrate to state an upper limit indicator for HO.

Volz et. al. (1979, 1981) tried to derive HO concentration by ground level measurements of ^{14}CO and ^{12}CO. Singh (1977) used the tropospheric concentration of methyl chloroform and other halocarbons with the same purpose. All these methods have many inherent uncertainties in their results. An understanding of the chemistry of the troposphere as well as a knowledge of the rate constants for the corresponding reactions must be known accurately in order to get reliable results.

Optical Absorption

This method involves the absorption of laser radiation by HO around 308 nm allowing the concentration to be estimated directly without the need for external calibration. Although apparently straightforward, this method has several drawbacks. This method loses sensitivity because it depends on the

quality of the photographic exposure, setting the detection limits around 2 x 10^6 HO molecules cm^{-3} in the best case. A second problem is the interference absorbance of other atmospheric species, e.g. SO_2, in the detection region. Stray sunlight, saturation of the HO transition and production of HO by the laser source are among other problems encountered.

Isotope Tracing - CO oxidation

This method is based on the measurement of oxidation rates of ^{14}C labelled CO by HO in an enclosed chamber. This is an absolute method since current atmospheric chemistry models state that more than 90% of the CO oxidation is carried out by reaction with hydroxyl radicals:

$$OH + CO \rightarrow CO_2 + H$$

From this equation we would expect the following rate expression:

$$d/dt\ [CO_2] = k\ [CO]\ [HO]$$

for $^{14}CO_2$

$$\frac{[^{14}CO_2]_t}{[^{14}CO]_o} = \frac{[^{14}CO_2]_o}{[^{14}CO]_o} + k'T$$

where $k' = k\ [OH]$

The rate constant for this reaction has been carefully determined by several investigators in previous studies. By using the ratio between ^{14}CO oxidized to the $^{14}CO_2$ produced as a function of time after ^{14}CO addition, the HO radical concentration can be derived.

This method encounters three major problems: (1) It is somewhat difficult to quantitatively collect the $^{14}CO_2$ formed, (2) there could be some production of $^{14}CO_2$ by other processes than the CO oxidation by HO, and (3) the chemistry can be perturbed by the walls of the reaction chamber.

Spin-Trapping

This method involves the trapping of hydroxyl radicals by a spin trapping reagent (4POBN). HO forms a stable adduct with 4POBN which can be determined by electron spin resonance and by gas chromatography/mass spectrometry. The success of the method depends on the efficiency of trapping, efficiency of extraction, loss of reagents by air pressure and possible loss of HO at the walls of the air sampling duct. The claimed detection limit of this method is 0.2×10^6 molecules cm^{-3}.

Laser Induced Fluorescence (LIF)

This technique involves the excitation of the hydroxyl radical by a tunable ultraviolet, uv, laser using one of the rotational lines in the $^2\pi(v''= 0) \rightarrow {}^2\Sigma(v'= 1)$ transitions and observing the fluorescence emission from the $^2\Sigma^+(v'= 1) \rightarrow {}^2\pi(v''= 1)$ transitions near 3145 Å or the $^2\Sigma^+(v'= 0) \rightarrow {}^2\pi(v''= 0)$ transitions near 3090 Å. This technique has great sensitivity and selectivity due to the high power laser sources and the fact that the fluorescence occurs shifted to the red end of the exciting radiation. The success of this method relies upon the

knowledge of the fluorescence spectrum and many physical and spectroscopical parameters involved in the absorption and emission processes. Several investigators have used variations of this technique to detect hydroxyl radical.

Atmospheric Pressure-Enclosed Chamber. Davis and co-workers used an airborne tunable dye laser focused into a fluorescence chamber into which outside air was drawn through a sampling duct. The enclosed chamber setting created doubt as to whether the concentration detected was representative of outside ambient air. Other problems encountered in this procedure were the interfering fluorescence of other species, the formation of HO by ozone dissociation and lack of appropriate calibration methods.

Atmospheric Pressure-Open Optical Arrangement. In order to eliminate possible HO loss at the walls of the chamber, Wang and co-workers tried an open optical arrangement. In this method a telescope observed fluorescence back scattered from outside the aircraft boundary layer after the outside air was electronically excited by the second harmonic of a tunable dye laser. Interference with ozone was also present in this measurement. Rayleigh scattered solar radiation produced background signal which obscured the real measurements.

The biggest problem encountered in atmospheric pressure measurements

was recognized by Chan et. al. (1983) when evidence of some pressure dependence was found in the quenching of the excited molecule by oxygen and water. It was found that the fluorescence efficiency is lower at atmospheric pressure than the calculated values at lower pressures.

Fluorescence Amplification with Gas Expansion (FAGE). In this method one attempts to eliminate most of the problems encountered in previous techniques. The outside air is drawn through a 1 mm orifice at the top of a 48 mm i.d. tube into the detection chamber which is maintained at a pressure of about 5 Torr. The expansion of the gas strongly discriminates against the formation of HO by the reaction of $O^1(D)$ with water vapor and against Rayleigh and Mie scattering. The background solar radiation is excluded from the detection chamber as it is in a contained environment. Although there is a drop in fluorescent molecules concentration due to the expansion, there is a comparable increase in fluorescence efficiency due to reduced quenching. This increase in fluorescence efficiency also results in a longer fluorescent lifetime allowing in this way the laser pulse to be separated from the detection signal. The measurement involves chemical modulation. A stream of isobutane is passed alternately through the orifice of the FAGE second nozzle as well as the first nozzle. Isobutane is used as an HO scavenger reducing the HO signal to 5% on the second tube. This value is used then as a background correction for the real HO measurements.

The interference of ozone is not completely suppressed, therefore it is convenient to find out the extent of ozone interference in such experimental setup. This interference comes about when the laser beam, passing through the detection chamber photolyses ozone producing $O^1(D)$. This highly reactive species can then react with water or with isobutane producing some more HO molecules, according to the reactions:

(1) $O_3 + h\nu \rightarrow O_2 + O^1(D)$

(2) $O^1(D)$ + water (H_2O) $\rightarrow HO^* + HO$

(3) $O^1(D)$ + isobutane $\rightarrow$ HO + isobutyl radical

In 1981 Davis et. al., stated that there is no thermalization of the HO molecules produced by ozone and water when the excitation is carried out at one atmosphere total pressure and that the interference in their measurements was not more than 25-50% depending on atmospheric conditions. Given the measurement procedure, it is also of interest to study the behavior and characteristics of the HO molecules potentially produced by the reaction of singlet oxygen with isobutane which contrary to the ozone-water case, are expected to have a thermal distribution. In order to do this, the rotational nascent distributions of HO from the three sources must be studied.

It is the purpose of this work to study the rotational distributions of the three sources i.e., natural atmospheric HO and the two spurious species (from the ozone-water, and ozone-isobutane reactions) and through them to gain a

better understanding of the interference of HO molecules produced by the detection and calibration methods on the detection of natural HO in the LIF technique using FAGE.

CHAPTER II

THEORY

ROTATIONAL-VIBRATIONAL STATES OF HYDROXYL RADICAL

The success of methods like LIF using FAGE for the determination of the concentration of hydroxyl radical depends on a thorough understanding of the rotational-vibrational energy levels of this molecule. In 1961 Dieke and Crosswhite updated the work of previous researches in the identification of HO bands (Table III) and calculated spectroscopical constants such as transitional probabilities (Table IV) and energies of the different rotational levels (Table V) of the ultraviolet bands of this molecule. The nomenclature and the constants used in this discussion refer to the ones stated by Dieke and Crosswhite (1961).

In the description of the rotational levels of this diatomic molecule the angular momentum K (disregarding the spin) will be used. This value is always an integer and it actually numbers the rotational states. In other papers it is also identified as N (Shardanand and Mohan 1975).

All the bands under study involve a single electronic transition. The lower state is the double degenerate ground state ^{2} and the upper level

TABLE III

IDENTIFICATION OF HO EXCITATION LINES

Wavelength	Wavenumber(cm^{-1})	1--->0	
2814.005	35526.83	$R_1$1	
2814.045	35525.59	$R_1$1'	
2815.368	35508.90	$R_1$10	
2815.558	35506.51	$R_1$10'	
2815.989	35501.08		$R_2$7
2816.024	35500.63		$R_2$6
2816.423	35495.61		$R_2$8
2816.549	35494.02		$R_2$5
2817.319	35484.31		$R_2$9
2817.380	34583.54	$R_1$11	
2817.580	35481.02	$R_1$11'	$R_2$4
2818.677	35467.22		$R_2$10
2819.145	35461.22	$Q_1$1,1' $R_2$3	
2819.822	35452.82	$R_1$12	
2820.045	35450.02	$R_1$12'	
2820.501	35444.29		$R_2$11

TABLE III

IDENTIFICATION OF HO EXCITATION LINES
(continued)

Wavelength	Wavenumber(cm^{-1})	1--->0
2820.669	35442.18	$Q_1 2$
2820.710	35441.66	$Q_1 2'$
2821.302	35434.22	$R_2 2$
2821.706	35429.14	$P_1 1$
2822.404	35420.38	$Q_1 3$
2822.466	35419.61	$Q_1 3'$
2822.705	35416.61	$R_1 13$
2822.787	35451.58	$R_2 12$
2822.953	35413.49	$R_1 13'$
2824.096	35399.17	$R_2 1$
2824.393	35395.45	$Q_1 4$
2824.455	35394.67	$Q_1 4'$

TABLE IV

TRANSITION PROBABILITIES FOR HO TRANSITIONS

K	P_1	Q_1	R_1	R_2
1	10.67	13.33	4.80	2.67
2	4.40	22.40	9.14	6.40
3	18.29	30.86	13.33	10.29
4	22.22	39.11	17.46	12.22
5	26.18	47.26	21.54	18.18
6	30.15	55.39	25.60	22.15
7	34.13	63.47	29.65	26.13
8	38.12	71.56	33.68	30.12

TABLE V

ROTATIONAL STATES OF HO IN WAVENUMBERS
V=0

K	f1	f1'	f2	f2'
1	00.00	00.03	126.43	126.12
2	83.70	83.90	187.71	187.47
3	201.90	202.37	289.01	288.83
4	355.09	355.87	429.45	429.23
5	543.54	544.82	608.15	608.16
6	767.45	769.17	824.49	824.76
7	1026.69	1029.10	1077.80	1078.47

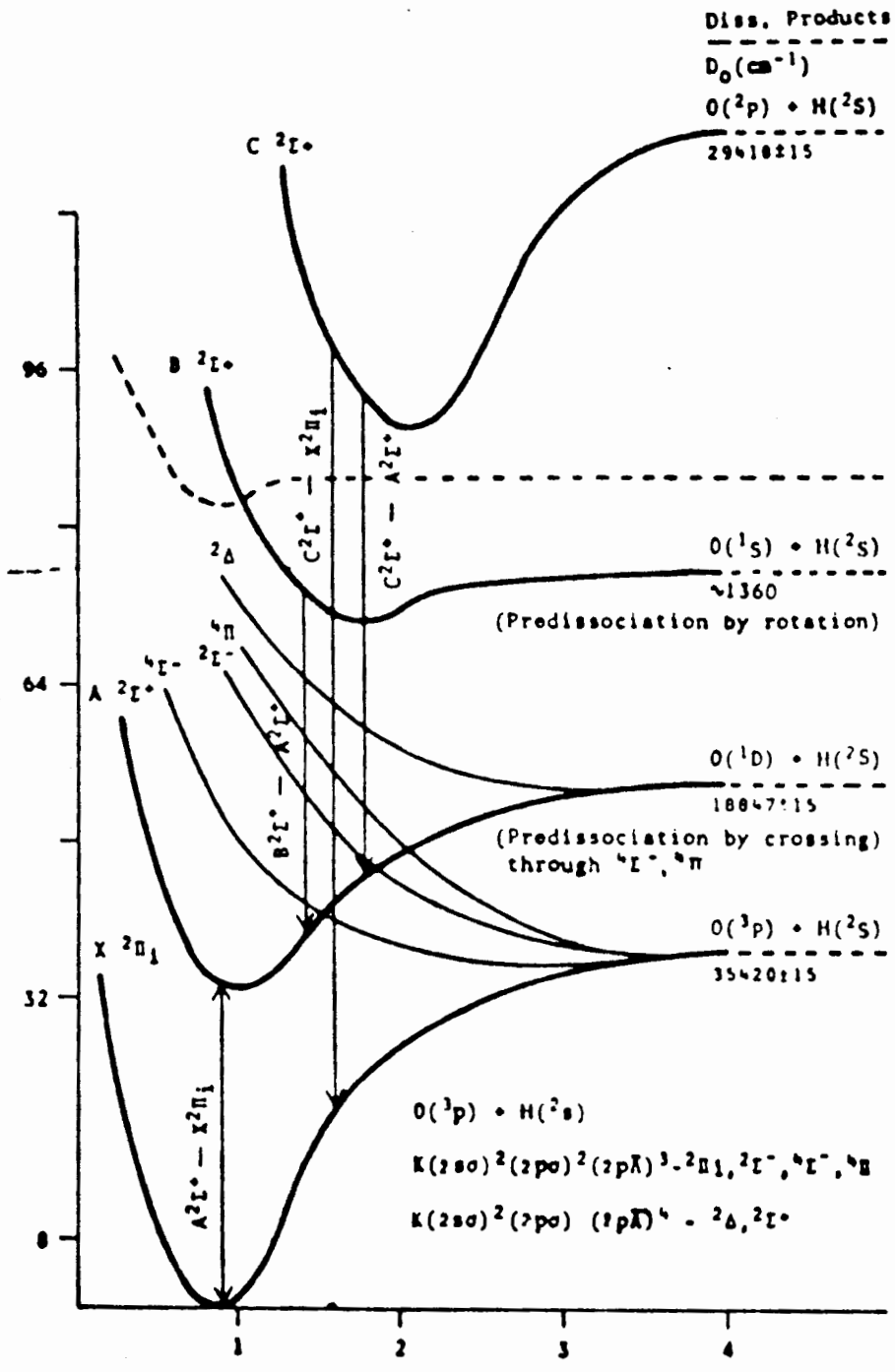

Figure1. Electronic levels and observed electronic transitions.

corresponds to the doubly degenerate $^2\Sigma+$ state (Figure 1, taken from Shardanand and Mohan 1975). There is almost no energy difference between the K=0 of the two Σ states (Figure 2, taken from Shardanand and Mohan). For higher values of K, there is an averaging of rotational energies and the resultant state has an energy equivalent to a $^1\Sigma$ state. For the ^{2} states there is a definite difference between the two states. This produces two sets of transitions. The first set from the $^2\pi_{3/2} \rightarrow {}^2\Sigma_{1/2}$ carries the subscript 1. The second set from the $^2\pi_{1/2} \rightarrow {}^2\Sigma_{1/2}$ carries the subscript 2.

The selection rules for these transitions are J → J and J$\pm$1 → J; K → K and K+1 → K, where the initial value is the higher state as in the the emission case. According to these selection rules we get 12 branches. The subscripts refer to the initial and final quantum number F'. The presence of only one subscript means the same initial and final F' state.

The 12 branches are:

O-branch for K-2 → K

$O_{12}(K)$= J-1 → J

P-branch for K-1 → K

$P_1(K)$= J-1 → J

$P_2(K)$= J-1 → J

$P_{12}(K)$= J → J

Q-branch for K → K

$Q_1(K)$= J → J

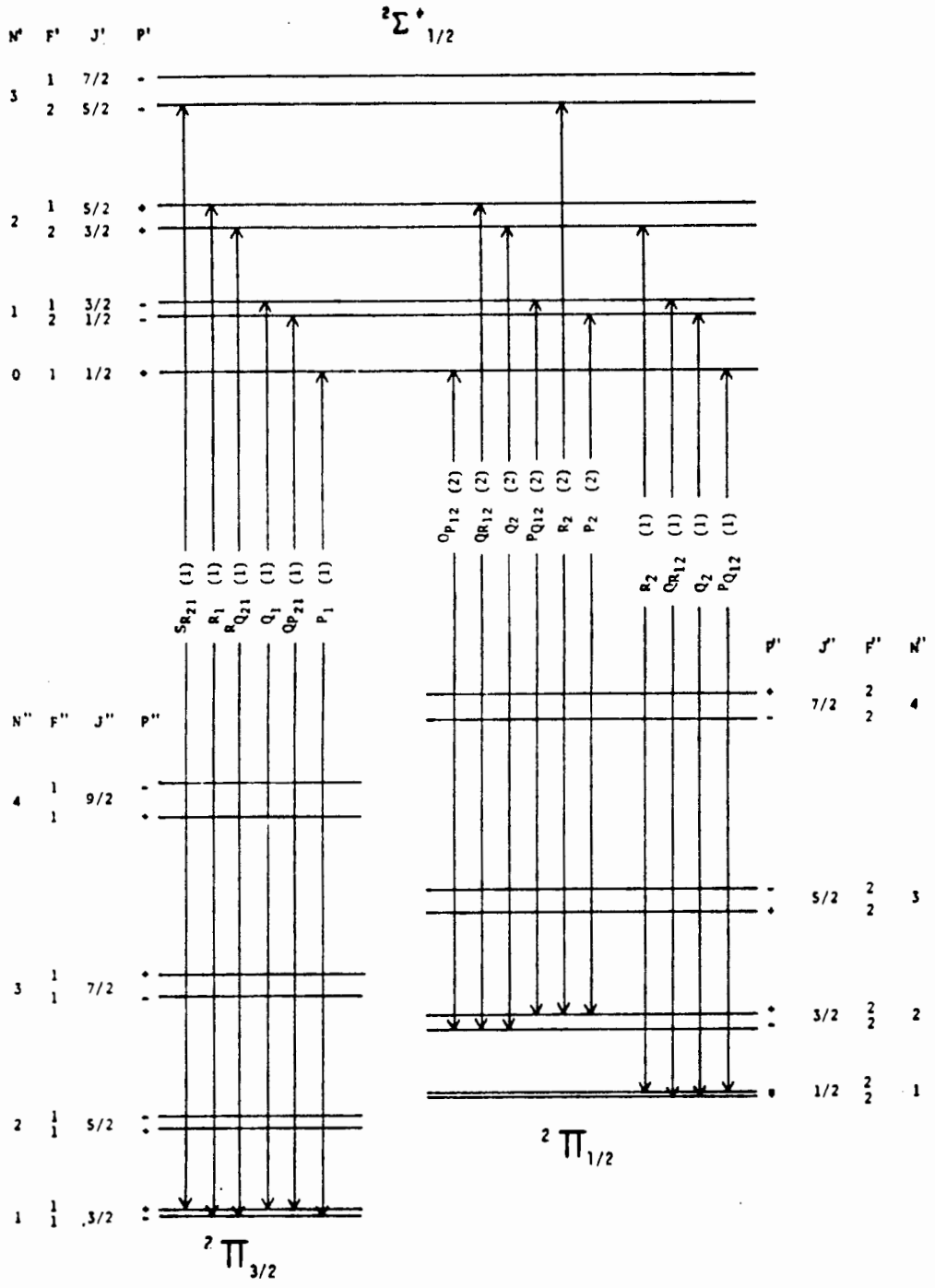

Figure 2. Branches of the rotational structure of HO.

$Q_{21}(K)= J-1 \rightarrow J$

$Q_2(K)= J \rightarrow J$

$Q_{12}(K)= J+1 \rightarrow J$

R-branch for $K+1 \rightarrow K$

$R_1(K)=J+1 \rightarrow J$

$R_{21}(K)=J \rightarrow J$

$*R_2(K)= J+1 \rightarrow J$

S-branch for $K+2 \rightarrow K$

$S_{21}(K)= J+1 \rightarrow J$

The transitions that obey both selection rules are called the main branches while the others are called the satellite branches (Figure 2). The transitions of main interest in this study are the ones belonging to the R_2 branch for reasons that will be discussed later. For our purposes, we will be looking at the fluorescence emissions around 309 nm from the absorption transitions around 281-282 nm, which enclose the lower K values of the R_2 branch, and parts of the Q_1, P_1 and R_1 branches.

BOLTZMANN DISTRIBUTION AND POPULATION LEVELS

The intensity of a line resulting from the transition of a molecule from a certain energy level K, depends on the population of the energy level:

$$(1) \quad I(K) = N(K) \times A(K) \times h\nu$$

where N(K) is the population at level K, A(K) is the transition probability from

level K, h is Planck's constant and ν is the radiation wavelength. When temperature equilibrium exists, the population of energy levels is controlled by the Boltzmann equation:

$$(2) \qquad N(K) = N_o \, e^{-E(K)/kT}$$

where N_o is a constant, E(K) is the energy associated with state K, k is the Boltzmann constant and T is the absolute temperature. If equation (2) is substituted into equation (1) we get:

$$(3) \qquad I(K) = N_o \, e^{-E(K)/kT} \times A(K) \times h\nu$$

Taking the natural logarithm on both sides of the equation and rearranging:

$$(4) \qquad \ln I(K) - \ln A(K) = \ln N_o \times \ln h\nu - E(K)/kT$$

or

$$(5) \qquad \ln I(K) - \ln A(K) = \text{constant} - E(K)/kT$$

From this equation we can see that with the intensity measurements and the appropriate energy and transition probability value, the absolute temperature can be determined from the inverse of the slope of a plot of (ln I(K) - ln A(K)) against E(K) (Figure 3).

Temperature measurements can give a great deal of information about the state of the molecules and about the mechanism by which the molecule was formed. In the case of LIF where there is interference of HO molecules produced by the photodissociation of ozone, temperature measurements of all three species (natural, ozone-water and ozone-isobutane) which actually indicate

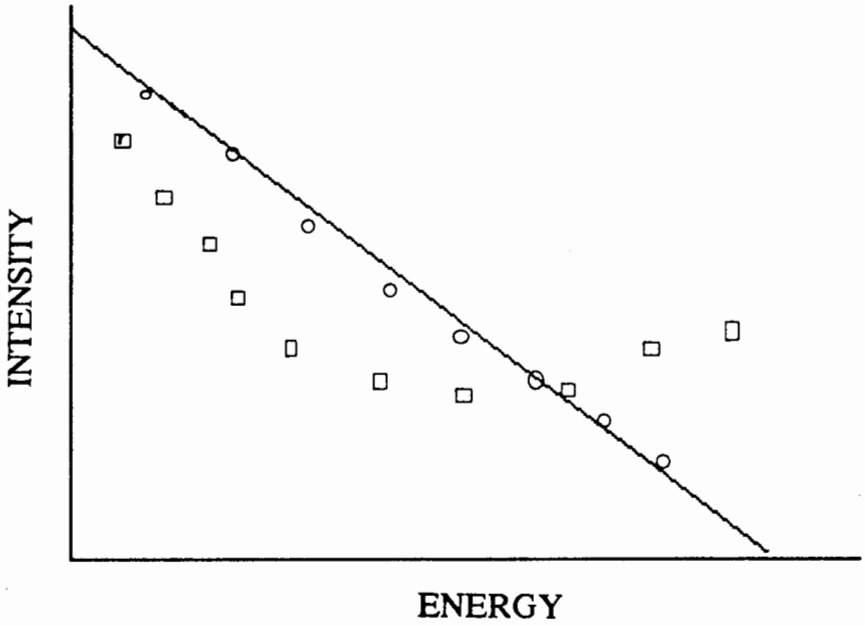

Figure 3. Sketch plot showing linearity and non-linearity of thermal and non-thermal population distribution.

the population distribution among the rotational energy levels, will indicate the level of interference of the laser produced hydroxyl radicals (ozone-water and ozone-isobutane). If all the molecules formed by laser photodissociation of ozone have the same rotational temperature as the naturally occurring HO, it means that both types of molecules occupy the same set of energy levels, and therefore their absorption characteristics will be the same, creating interference. If, on the other hand the energy levels of the ozone produced HO have different rotational energy level population i.e., different rotational temperature, the molecules will not absorb the laser energy to the same extent, therefore less interference with the naturally occurring HO will be present. The level of interference can be determined by plotting population of level K versus the energy of level K, for all K values (Figure 4). The ratio of the percent population for the K level of the photolytic HO, to the percent population for the K level of natural occurring HO, is the level of interference. Even though all the K levels cannot be measured with the present technique, with the appropriate temperature measurements the level of interference of laser produced HO can be assessed.

TEMPERATURE MEASUREMENTS

As stated before, a knowledge the rotational temperature of the different species of HO present in the LIF experiments will indicate the level of interference of laser produced HO with the detection of the naturally occurring

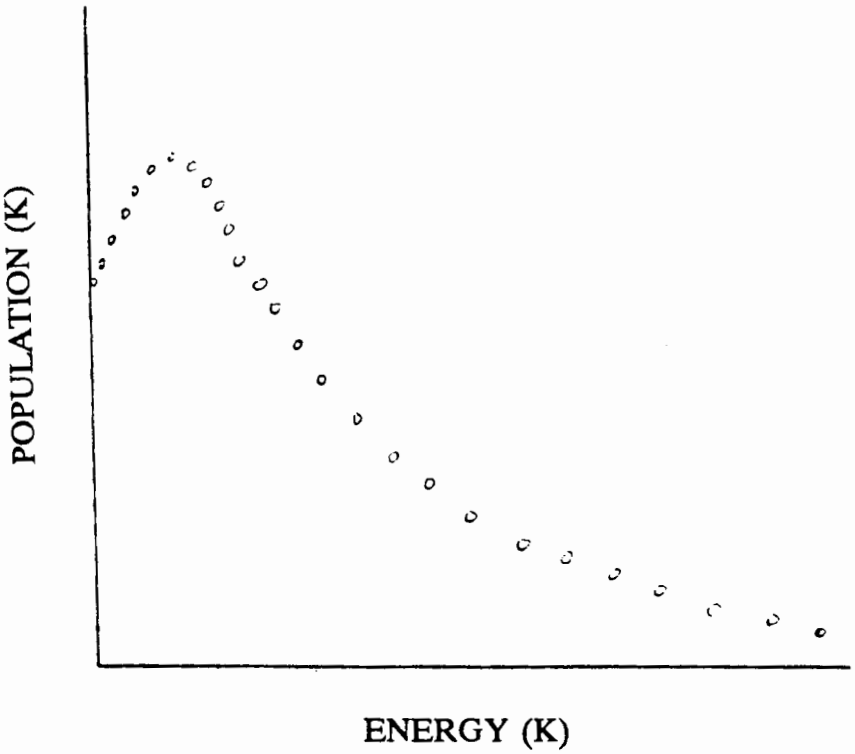

Figure 4. Sketch plot of population of level K versus energy of level K.

species. It is expected that the ozone-water produced HO will have a different rotational distribution because it was produced by the reaction of the highly energetic $O^1(D)$ with water vapor. In this reaction two molecules of HO are produced and according to Gericke et al. (1980) and Rodgers et al. (1981), only one of the molecules is energetically "hot". According to these researchers the "hot" HO is the one produced by the formation of new bond between the $O^1(D)$ and the H atom in the water molecule. Since the other HO molecule results from a shift of the hydrogen atom out of the water molecule it is not "hot" and according to their studies it has a thermal distribution, in the same range as the natural occurring HO, therefore this is the one that causes the interference in the LIF experiments.

The ozone-isobutane produced HO is expected to have a thermal distribution. According to Luntz (1980), there are two mechanisms for the HO formation through the reaction of hydrocarbons with $O^1(D)$: insertion and abstraction.

The abstraction pathway is favored as the number of carbons in the hydrocarbon molecule increases. This pathway produces a statistical or thermal population while the insertion pathway does not. In the case of isobutane the abstraction pathway is expected to be favored, so a statistical distribution is also expected.

In choosing which branch of the vibrational-rotational spectrum to monitor and calculate intensities, certain factors have to be taken into

consideration. The first factor to consider is the superposition of other lines. They should be single lines free of satellites, otherwise the calculation of the intensities gets much more complicated. The last factor to consider is the proximity of the lines of interest. In our case we can only scan 2 nm at a time without having to readjust the dye laser system. This means that the branch chosen must have several detectable lines within a 2 nm distance. The R_2 branch meets all of these requirements. In the first place they are single lines, considerably isolated from neighbor lines and second, there are about 6 lines detectable by our system in less than 2 nm ie., from 281.4 to 282.5 nm.

CHAPTER III

EXPERIMENTAL

The experiment consisted of three parts: the collection of the excitation spectrum of the naturally occurring HO, the collection of the excitation spectrum of the laser produced HO by the reaction of $O^1(D)$ with water vapor and by the reaction of $O^1(D)$ with isobutane. The methods of laser excited fluorescence with amplification through gas expansion were used in these collections. The results from these experiments were compared to direct gas temperature measurements made using a thermocouple inside the probe nozzle and tube. As discussed in previous sections the LIF method involves inducing the transition from the $^2\pi \rightarrow {}^2\Sigma$ electronic state by absorption of light around 282 nm and observing the consequent fluorescence around 309 nm. A scheme of the experimental setup for the LIF experiments is presented in Figure 5.

LASER SYSTEMS

The laser systems used in these experiments are novel for this purpose. This is the first time that we use a copper vapor laser for the pumping of a

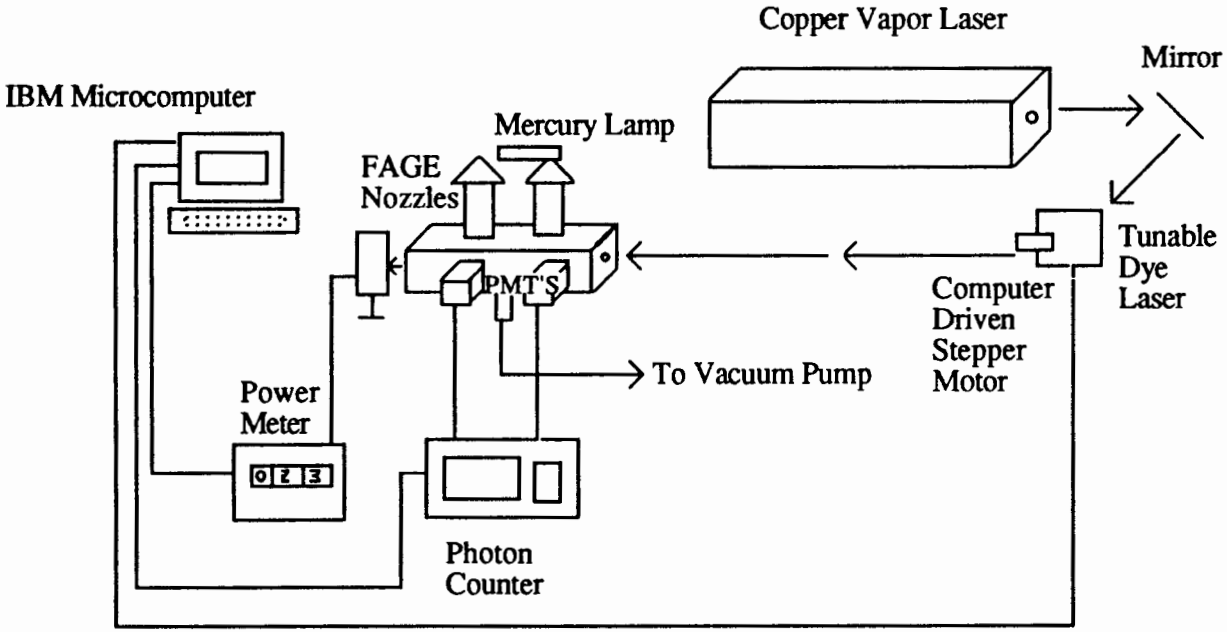

Figure 5. Scheme of the experimental setup.

tunable uv dye laser. In previous studies (Chan et. al. 1983, Wang et. al. 1981 and Davis et. al. 1976) the desired frequency around 282 nm was obtained by a frequency doubled Rh6G dye laser pumped by a frequency doubled Nd-YAG laser.

The new system was designed to produce pulses with lower energy while maintaining the high average power observed in the Nd-Yag system. This was desired in order to avoid saturation and reduce photolytic interference in HO concentration measurements since the photolytic interference is proportional to the square of the laser pulse energy. Also the development of a more compact dye laser system was desirable for future measurements from an aircraft.

The old laser system required doubling the wavelength twice to produce 282 nm, once after the output of the Nd-Yag laser and again after the 564 nm output from the dye laser. The energy per pulse was 0.6 mJ, 6.7 ns full width at half-maximum (FWHM), 0.3 cm^{-1} FWHM performing at a rate of 30 Hz.

The new copper vapor model 251 from Metalaser Incorporated, produces a green light at 511 nm which is directly absorbed by our newly designed dye laser. The dye laser produces a line around 564 nm which is doubled by a Beta Barium Borate doubling crystal to produce the desired wavelength around 282 nm. The tuning of the device is achieved by means of two gratings. The first grating is parallel to the incident beam (grazing incident angle grating) and it is stationary. The second grating is a Littrow grating (at an angle to the incident light, about 45°) and this one is rotated by a computer controlled

stepper motor to tune the laser to the desired wavelength. The average energy per pulse obtained with this system is 9 x 10^{-4} mJ, 17 ns full width at half maximum, .3 cm^{-1} FWHM performing at a rate of 5.6 KHz.

FAGE INSTRUMENT

The FAGE instrument is a major modification of the one described by Hard et. al. (1984). The instrument consists of a sampling probe with nozzle of 1mm diameter which admits the air flow into a 48 mm i.d. cylindrical tube 0.35 m long allowing in this way the gas expansion. The interior of the nozzle and the tube are coated with a halocarbon wax in order to minimize loss of HO at the walls. The tube leads the air flow into the fluorescence cell through which the laser beam passes transversely and a pressure of about 4 Torr is maintained. The pressure is controlled by means of a large valve connected to a vacuum pump.

HYDROXYL RADICAL SOURCES

In the first part of the experiment where the excitation spectra of naturally occurring hydroxyl radicals were being measured, high concentrations of the molecule were produced by 185 nm photolysis of water vapor under a mercury lamp with quartz windows. The gas outlet of the lamp was placed

directly on top of the nozzle opening on the FAGE instrument (Figure 6).

For the second set of experiments, where the ozone-produced HO was being monitored, high concentrations of ozone (about 30 ppm) were produced by an ozone generator. The ozone, flowing at a rate of 3 - 5 liters per minute was then mixed at the adapted nozzle inlet with water saturated air produced by bubbling 7 liters of dry air per minute through water at 18°C. A total gas flow of 12 liters per minute was delivered to the exterior of the nozzle inlet, of this flow 8 liters per minute passed through the nozzle.

For the third part of the experiments the same setup for the ozone was used except that the gas was not mixed with water but with a stream ofisobutane directly into the nozzle inlet.

DETECTION SYSTEM

The fluorescent radiation was observed through a side window on the fluorescence cell. A pair of lenses, with a 3 nm FWHM band pass filter centered at 309 nm between them, focused the radiation onto a mask in front of the PMT (photomultiplier tube), positioned at 90° to the laser beam. The output from the PMT was then amplified by a variable gain amplifier model 777 from Phillips Scientific. Photon pulses in the amplified signal were converted to digital pulses by a Phillips Scientific NIM discriminator model 704. The resulting square wave pulses were counted by a Tennelec 532 pulse counter. The pulse

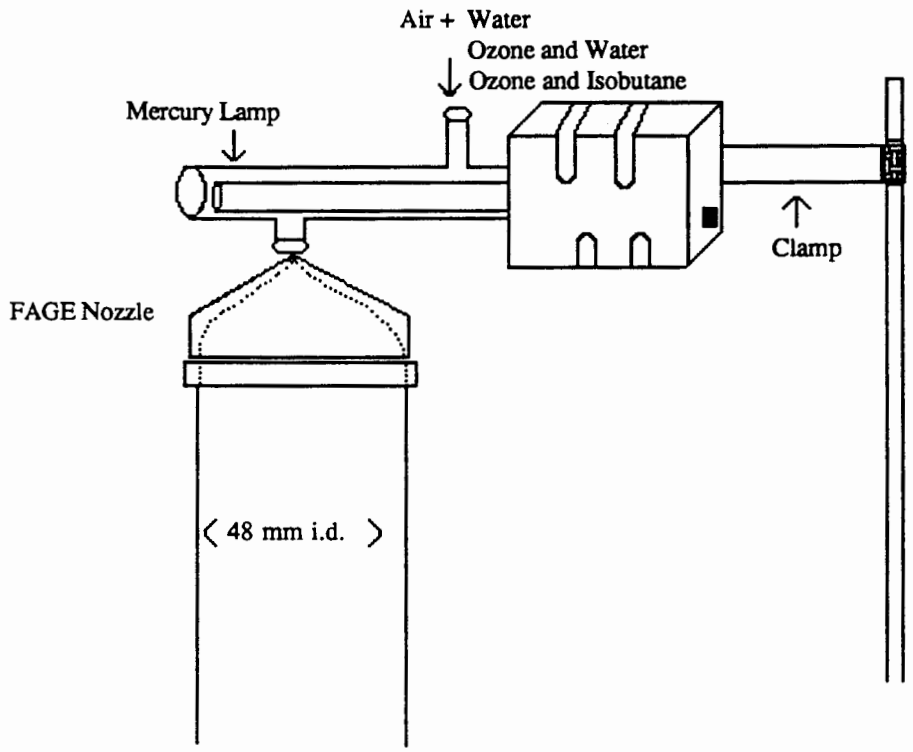

Figure 6. FAGE nozzle. Figure shows adaptation for mercury lamp.

was interfaced with an IBM-AT personal computer which stored the data. The laser power was monitored by a power meter positioned at the end of the fluorescence chamber perpendicular to the laser beam. The output from the power meter was also stored in the computer and the pulses counted were normalized to this value.

The tuning of the dye laser was accomplished by rotating one of the gratings in the laser using a micrometer controlled by a computer driven stepper motor. The computer program allowed flexibility in the resolution by controlling how often the readings from the pulse counter and the power meter were taken. In most cases the program was set to take readings for 10 seconds every 10 stepper motor steps. This allowed readings every 0.078 cm^{-1} since 600 steps completed one micrometer turn and each turn covered 4.70 cm^{-1}.

IDENTIFICATION OF LINES

The stepper motor was used to scan the doubled dye laser through the excitation spectrum. A graph of normalized counts ie. counts/uv laser power, was plotted against micrometer steps. The resulting graph is presented in Figure 7. The line pattern was compared with previous HO excitation spectra and referenced to the absorption spectra of Dieke and Crosswhite.

The linewidth of our laser was measured by measuring the distance between two isolated well identified lines, and their widths. For this purpose the

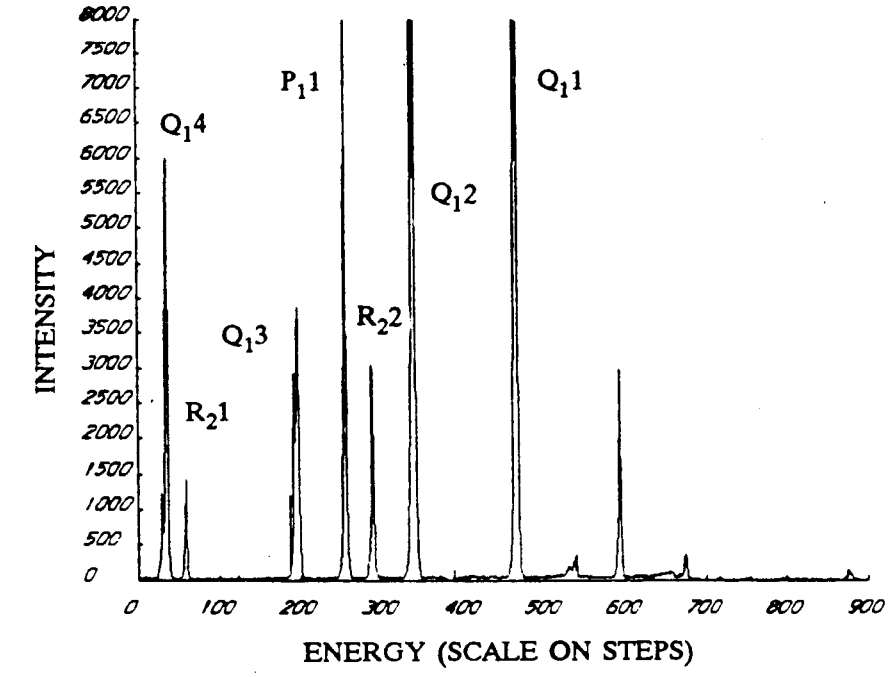

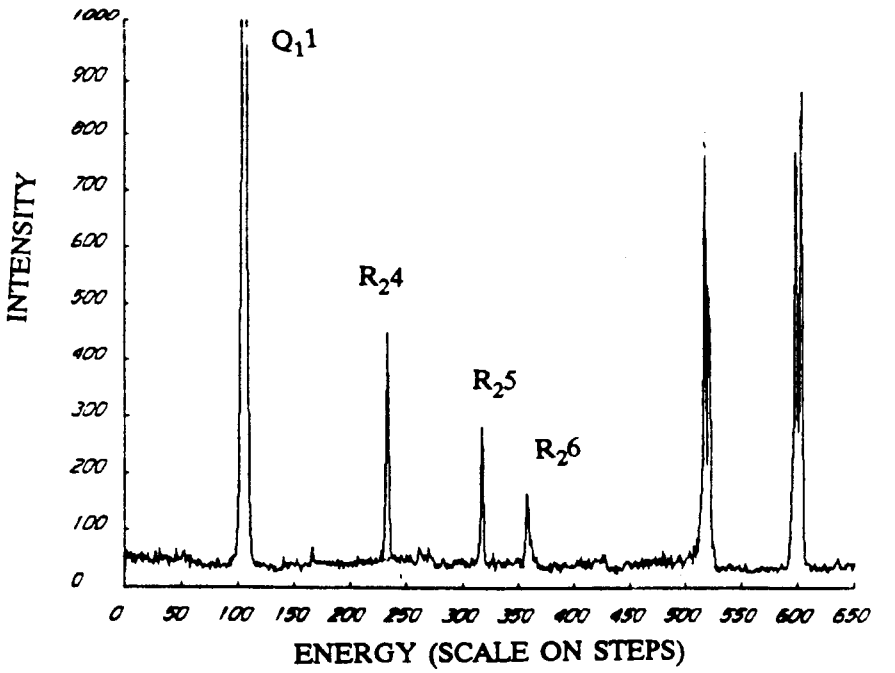

Figure 7. Line identification spectra. Horizontal axis is an arbitrary "steps" scale representing the energy of transition. Vertical axis indicates signal intensity.

$R_2 2$ line at 35434.22 cm^{-1} and the $P_1 1$ line at 35429.14 cm^{-1} were chosen (Figure 8). The difference between these lines in step units and in inches on plotted spectra was measured and ratioed to the difference in cm^{-1} between the same lines in Dieke and Crosswhite (1961). The FWHM was then measured in inches using the $P_1 1$ line and then the value was converted to cm^{-1}. The resulting FWHM was .25 cm^{-1}. With the proper conversion factors our steps scale was calibrated to a cm^{-1} scale and the spectrum replotted (Figure 9). Complete identification of the lines was achieved by comparison with values from Table III.

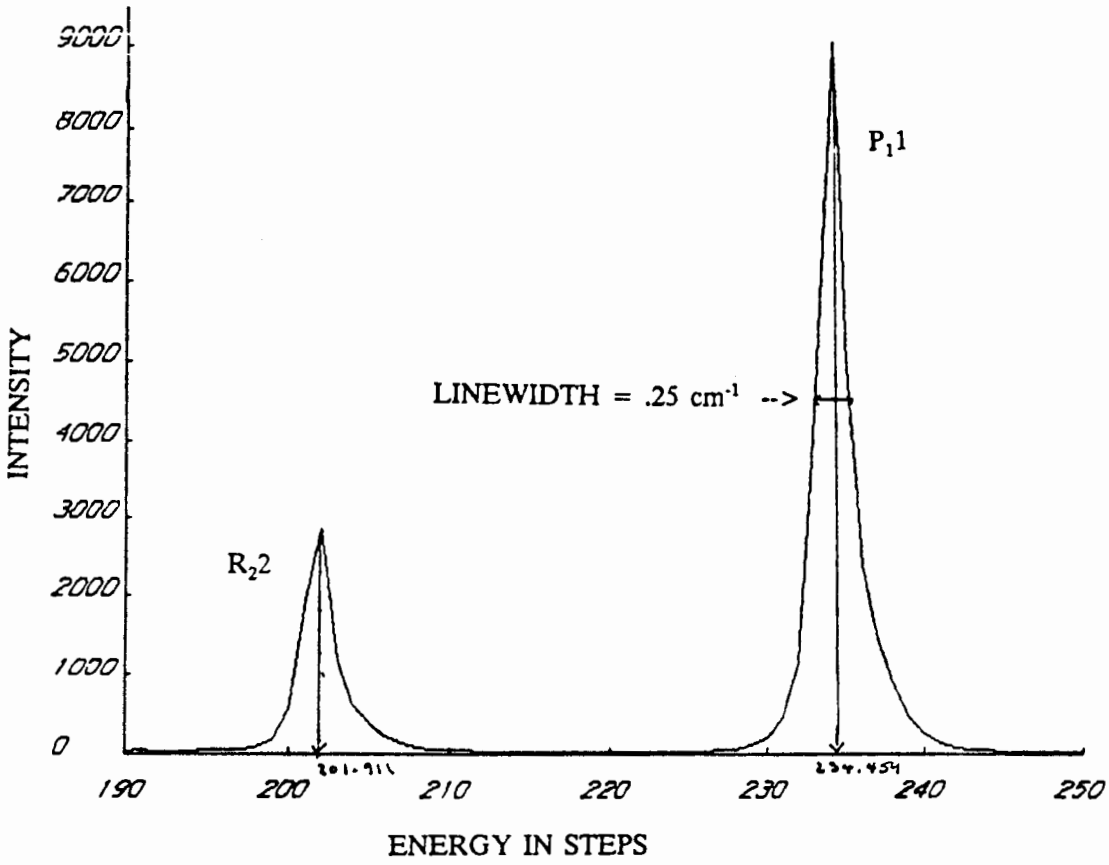

Figure 8. Linewidth measurements. The $P_1$1 line at 35429.14 cm^{-1} and the $R_2$2 line at 35434.22 cm^{-1} were used for linewidth measurements.

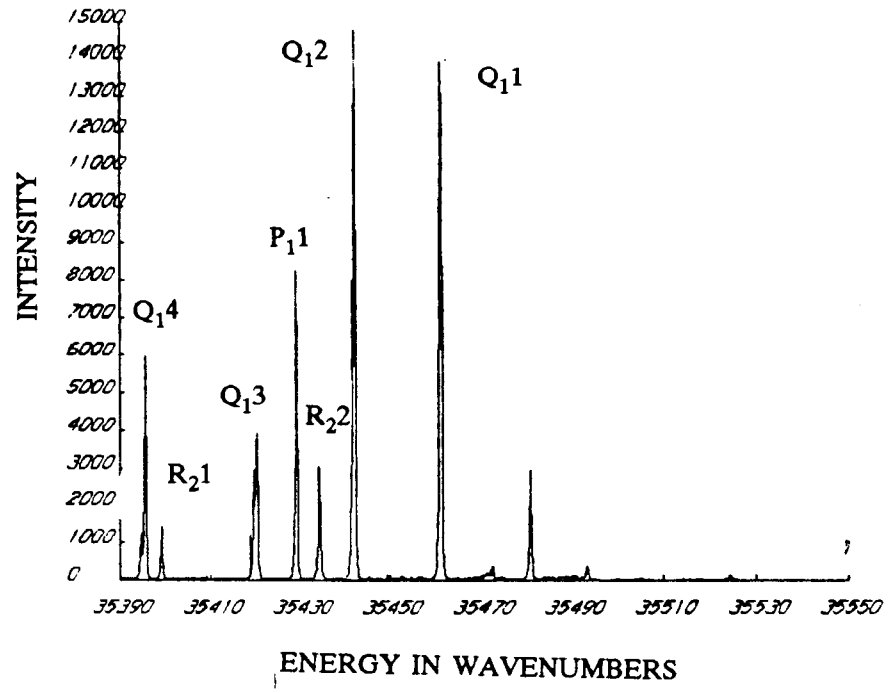

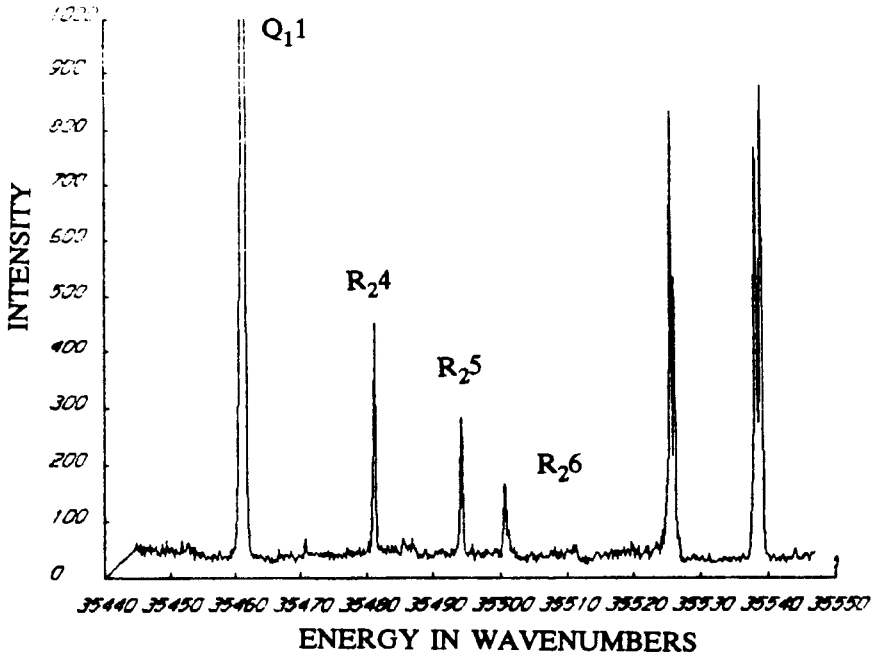

Figure 9. Line identification spectra in wavenumbers. Same spectra as in figure 7, but with the horizontal axis corrected to wavenumbers.

CHAPTER IV

RESULTS

COLLECTION OF SPECTRA AND LINE IDENTIFICATION

The $Q_1 1$ line appeared approximately in the center of the area of the spectrum under study. For this reason on first trial the uv laser power was tuned for a maximum at the $Q_1 1$ line hoping that it would not drift too much throughout the region of interest. However, this method did not work because the laser power continually decreased as we moved away from the $Q_1 1$ line. To keep the power constant, continuous adjustments of the optical system were required. In many cases the experiment had to be stopped and the low pressure fluorescence cell had to be opened to clean the deposits from the inside windows. For these reasons the experiments lasted many hours and it was impossible to collect the whole spectrum in one day's experiment.

The second approach was to adjust the laser power to a maximum output at one end of the spectrum and record from there to the $Q_1 1$ line concluding in this way one set of data. For the second part, the laser power was readjusted at the $Q_1 1$ line to cover the other half of the spectrum. The obtained intensities

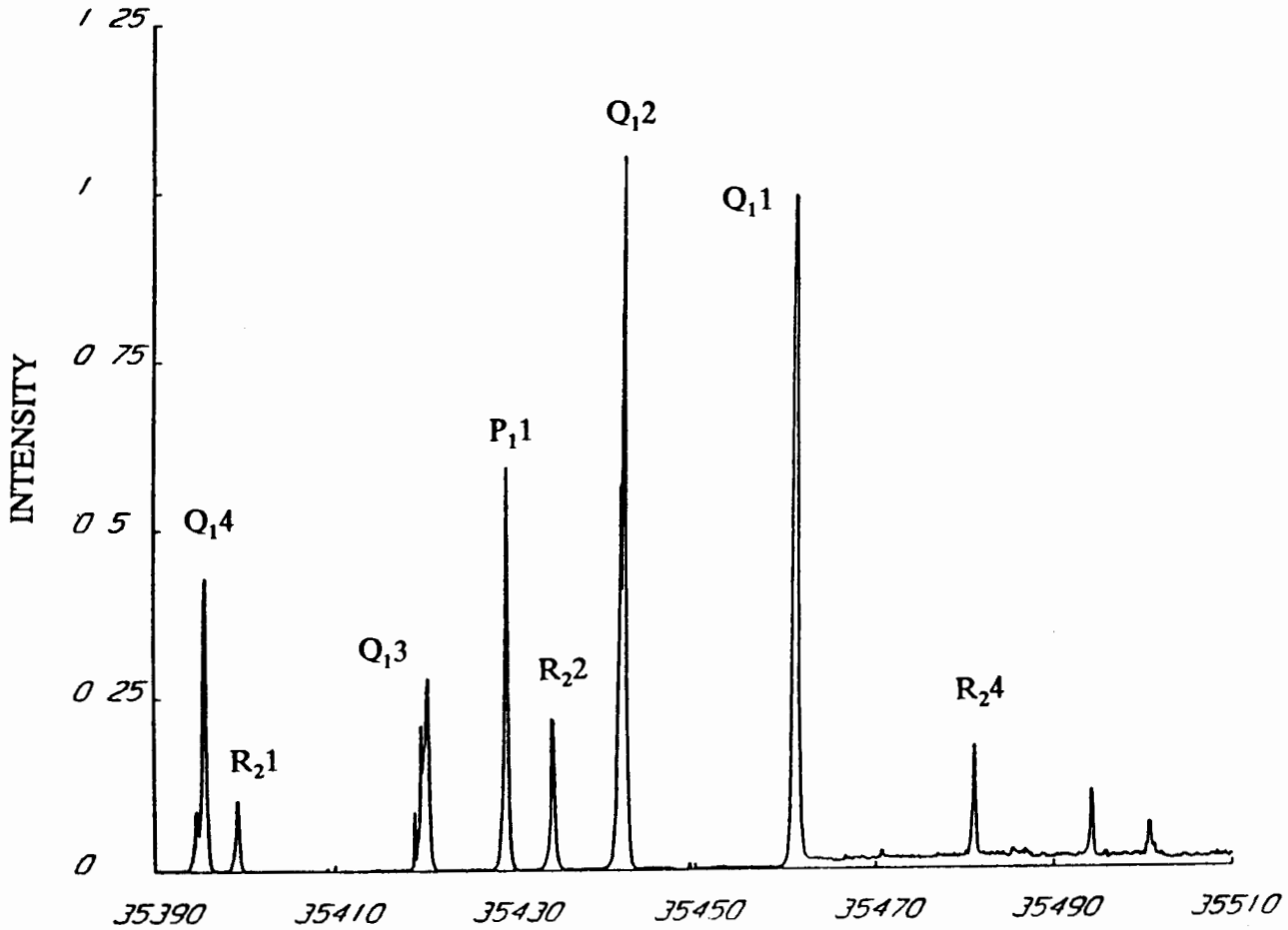

Figure 10. Hydroxyl radical spectrum. Spectrum is the product of merging two sets data for natural HO, left and right of the $Q_1 1$ line. Horizontal axis represents energy in wavenumbers and the vertical axis is the intensity of the transition.

were normalized by the common line in both sets of data. The final resulting spectrum is presented in Figure 10.

The same procedure was used to collect the HO spectrum from the ozone-water reaction and this is presented in Figure 11. For the ozone-isobutane case only the lines of interest were scanned so the spectrum of the whole region is not presented.

Identification of the lines was accomplished by comparing the literature values for the transitions with the actual experimental peaks. These numbers are reported for mercury lamp HO and for ozone-water HO in Tables VI and VII respectively. For the ozone-isobutane case the micrometer was already calibrated from the previous experiments, therefore it was not necessary to obtain the whole spectrum in order to identify the lines correctly.

LINE INTENSITIES

The intensities of the various $R_2(K)$ lines were determined by the peak height and also by the area under the curve for the ozone cases. In order to compare intensity values from the two different data sets in each experiment, the values were normalized by the common line in both sets. For the natural HO experiment both data sets were normalized by the $Q_1 1$ intensity. For the ozone-water HO the values were normalized by the $Q_1 3$ line intensity. The values for the ozone-isobutane HO did not have to be normalized because the

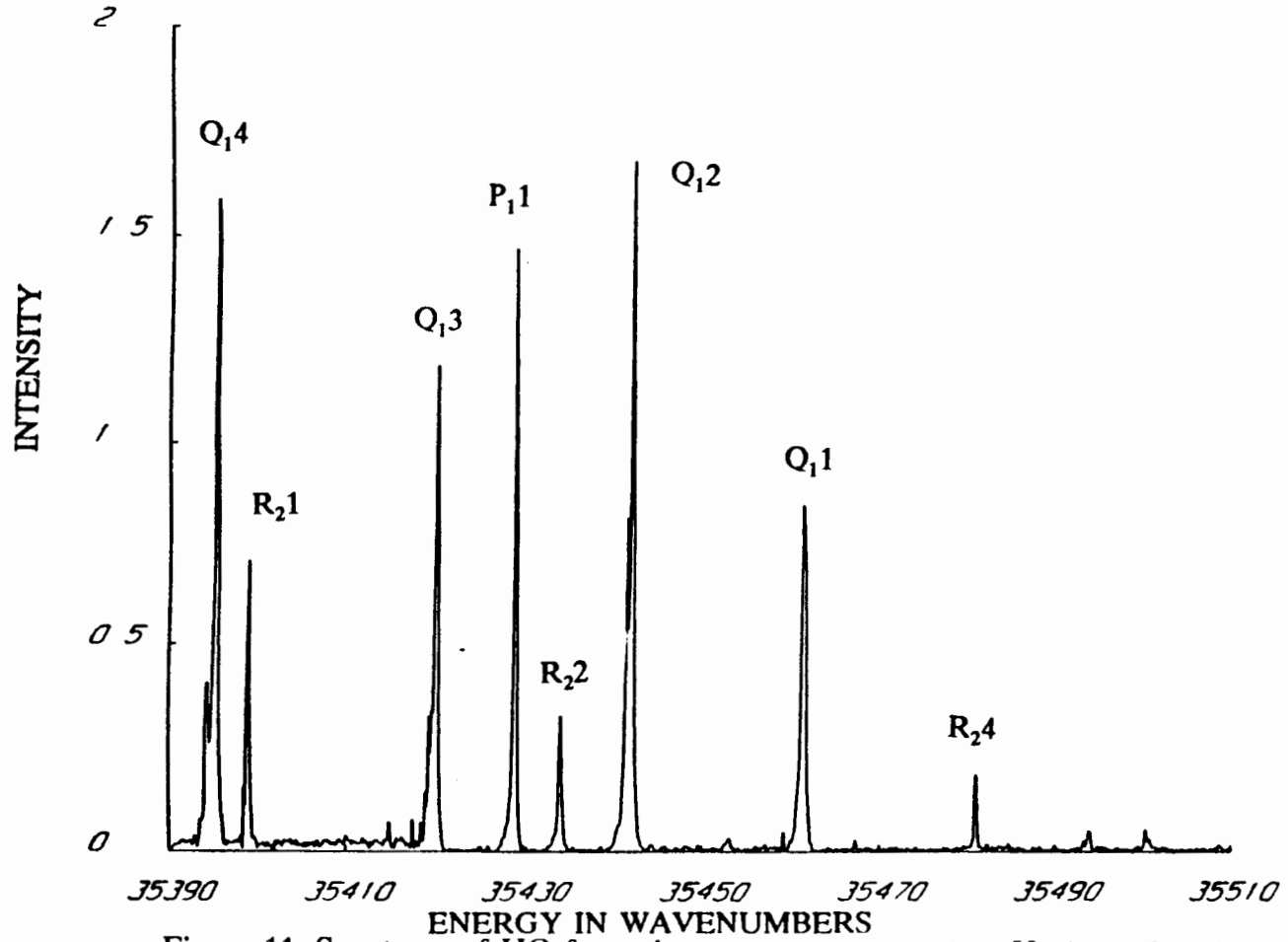

Figure 11. Spectrum of HO from the ozone-water reaction. Horizontal scale is the energy in wavenumbers. Vertical axis represents intensity of the transition. Spectrum is the product of merging two data sets,left and right of the $Q_1 3$ line.

peaks were scanned during the same experiment. The resulting values are presented in Tables VIII, IX and X for the naturally occurring HO, the ozone-water and the ozone-isobutane produced HO, respectively. For the ozone-water case the results obtained just from one set of data (excluding the R_21 line) are also presented to corroborate the temperature measurements. These results are presented in Table XI.

TABLE VI

COMPARISON OF EXPERIMENTAL DATA FOR HO TRANSITIONS WITH LITERATURE VALUES

Transition	Dieke et.al.(1969)	Experimental	difference
$Q_1 4'$	35394.67	35394.58	+.09
$Q_1 4$	35395.45	35395.65	-.20
$R_2 1$	35399.17	35399.17	.00
$Q_1 3'$	35419.61	35419.67	-.06
$Q_1 3$	35420.38	35420.45	-.07
$P_1 1$	35429.19	35429.18	+.01
$R_2 2$	35434.22	35434.22	.00
$Q_1 2'$	35441.66	35441.88	-.22
$Q_1 2$	35442.18	35442.35	-.17
$Q_1 1$	35461.33	35461.33	.00
$R_2 4$	35481.02	35481.21	-.19
$R_2 5$	35494.02	35494.19	-.17
$R_2 6$	35500.63	35500.61	+.02

AVERAGE = -.07

STD.DEV = $\pm$.1

TABLE VII

COMPARISON OF EXPERIMENTAL DATA FOR SPURIOUS HO TRANSITIONS WITH LITERATURE VALUES

Transition	Dieke et.al.(1969)(cm^{-1})	Experimental(cm^{-1})	difference
$Q_1 4'$	35394.67	35394.36	+.31
$Q_1 4$	35395.45	35395.29	+.16
$R_2 1$	35399.17	35399.02	+.15
$Q_1 3'$	35419.61	35419.36	+.25
$Q_1 3$	35420.38	35420.23	+.15
$P_1 1$	35429.19	35428.09	+.10
$R_2 2$	35434.22	35434.22	.00
$Q_1 2'$	35441.66	35441.68	-.02
$Q_1 2$	35442.18	35442.31	-.13
$Q_1 1$	35461.33	35459.43	+.10
$R_2 4$	35481.02	35481.03	-.01
$R_2 5$	35494.02	35493.93	+.09
$R_2 6$	35500.63	35500.31	+.32

AVERAGE = +.11

STD.DEV = $\pm$.13

TABLE VIII

EXPERIMENTAL HO LINE INTENSITIES

All values normalized to the $Q_1 1$ line.

K	intensity	ln intensity
Values normalized to laser power.		
1	.103	-2.28
2	.219	-1.52
**4	.214	-1.54
4	.179	-1.72
5	.192	-1.65
6	.066	-2.72
Values not normalized to laser power.		
1	.173	-1.75
2	.316	-1.15
**4	.357	-1.03
4	.148	-1.91
5	.112	-2.19
6	.0534	-2.93

** This value for $R_2 4$ belongs with the $R_2 1$ and $R_2 2$ set of data.

TABLE IX

EXPERIMENTAL HO LINE INTENSITIES FOR THE OZONE-WATER REACTION

All values normalized to the $Q_1 3$ line.

K	intensity peak height	intensity integral	ln intensity peak height	ln intensity integral
Values normalized to laser power.				
1	.775	.501	-.255	-0.691
2	.273	.289	-1.30	-1.24
*3	----	----	-----	-----
4	.119	.399	-2.13	-2.70
5	.042	.0672	-3.17	-2.70
6	.044	.0789	-3.12	-2.54
Values not normalized to laser power.				
1	.707	.734	-.347	-.307
2	.442	1.029	-.816	.029
*3	----	-----	-----	-----
4	.046	.284	-3.08	-1.26
5	.031	.150	-3.47	-1.90
6	.026	.221	-3.65	-1.51

* $R_2 3$ line indistinguishable from the $Q_1 1$ line.

TABLE X

EXPERIMENTAL HO LINE INTENSITIES FOR THE OZONE-ISOBUTANE REACTION

K	intensity peak height	intensity integral	ln intensity peak height	ln intensity integral
Values normalized to laser power.				
1	46.54	8.43	3.84	2.13
2	65.27	21.83	4.18	3.08
*3	-----	-----	----	----
4	48.85	15.74	3.89	2.76
5	16.76	8.76	2.82	2.17
Values not normalized to laser power.				
1	377	68.35	5.93	4.22
2	359	127.99	5.88	4.85
*3	---	-----	----	----
4	142	48.09	4.96	3.87
5	57	26.34	4.04	3.27

* $R_2 3$ line undistinguishable from the $Q_1 1$ line.

TABLE XI

EXPERIMENTAL HO LINE INTENSITIES FOR THE OZONE-WATER REACTION WITHOUT THE R_21 TRANSITION

K	intensity		ln intensity	
	peak height	integral	peak height	integral
Values normalized to laser power.				
2	105.4	24.78	4.65	3.12
4	46.1	25.03	3.83	3.22
5	16.3	5.21	2.79	1.65
6	17.1	6.17	2.84	1.82
Values not normalized to laser power.				
2	801	148.41	6.69	5.00
4	83	40.85	4.42	3.71
5	57	21.54	4.04	3.07
6	48	31.82	3.87	3.46

TEMPERATURE DETERMINATION

The temperature was determined by plotting the natural log, ln, of the intensity minus the natural log, ln, of the transition probabilities versus the state energy in cm-1 scale. The slope of this plot gives -1/kT where k is the Boltzmann constant in cm^{-1} units.

$$k = 1.38 \times 10^{-23} JK^{-1} \times [(6.6 \times 10^{-34} Jsec)(3.0 \times 10^{10} \text{ cm sec}^{-1})]^{-1}$$

$$= 0.697 \text{ cm}^{-1}k^{-1}$$

So, if the slope is multiplied by 0.697 $cm^{-1}K^{-1}$, the inverse of this product is the absolute temperature. The plots of these graphs are presented in Figures 12, 13a, 13b and 14 for the three cases respectively. The obtained temperature values are presented in Table XII.

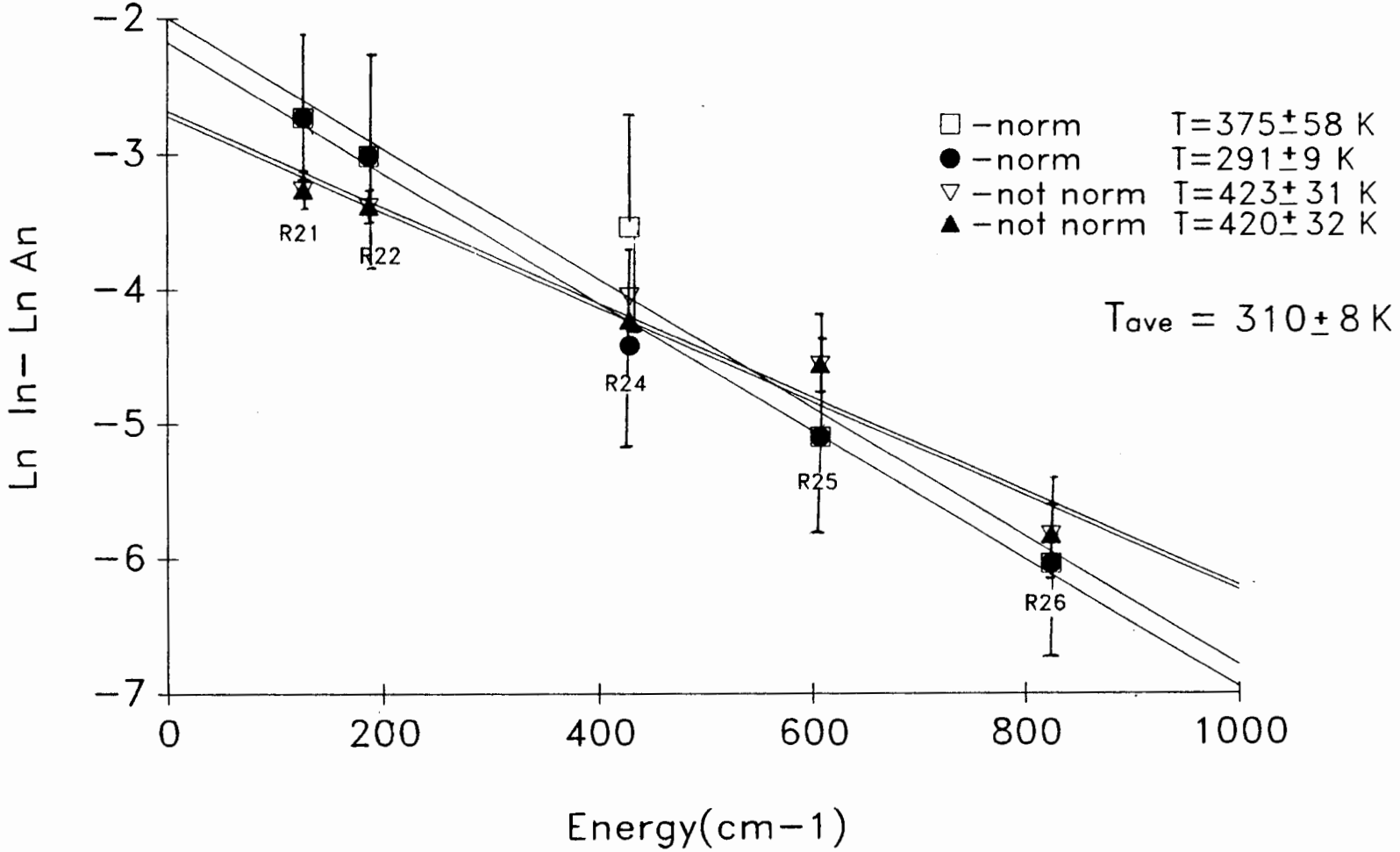

Figure 12. Plot of intensity of natural HO versus energy. The inverse slope of this plot is the product of the absolute temperature and the Boltzmann constant and it was used to determine it. The four cases represent different ways of analyzing the data.

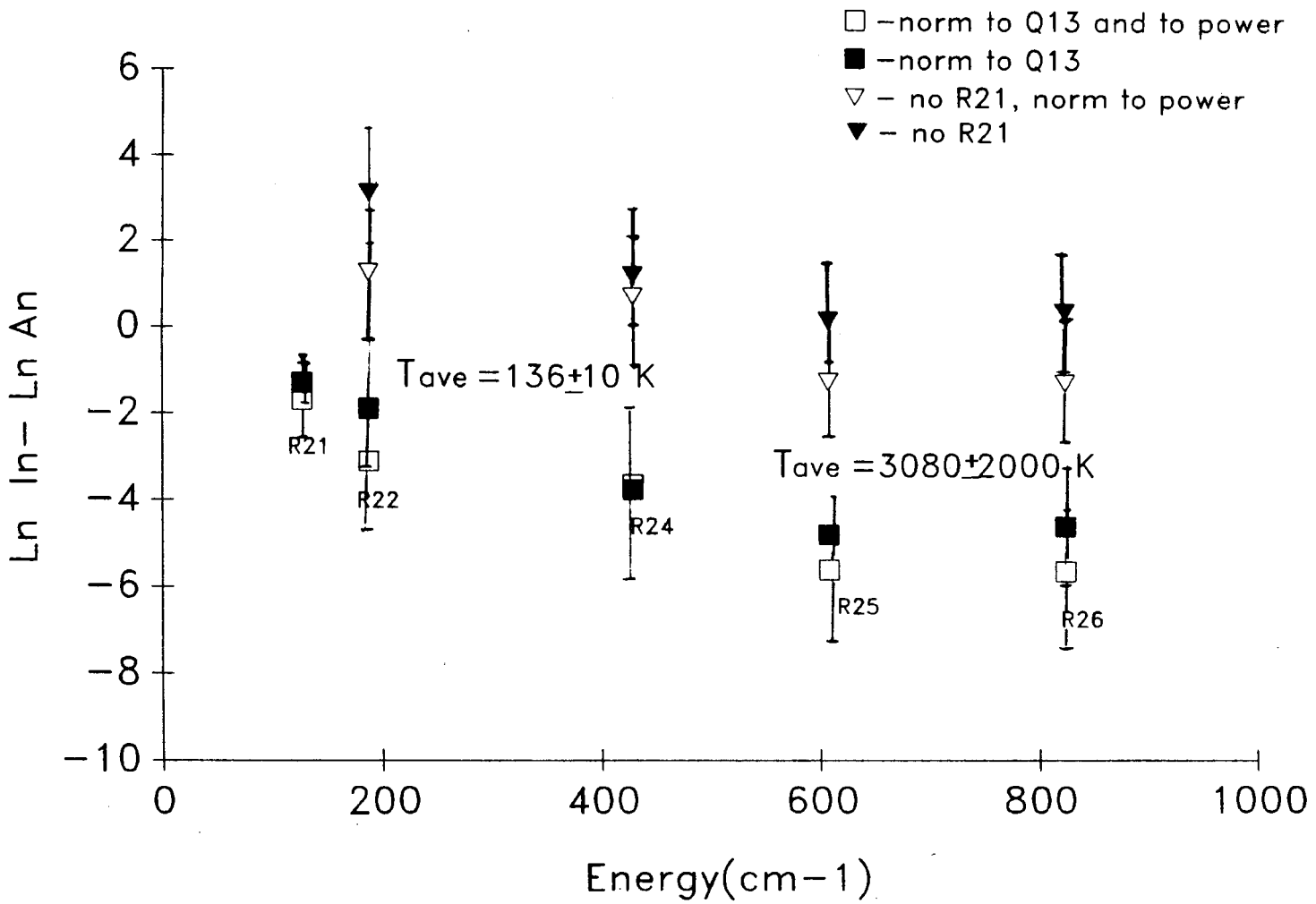

Figure 13a. Plot of intensity of HO from the ozone-water reaction versus energy. The intensity value was taken from the area under the curve. As in figure 12, from the inverse of the slope the temperature value was calculated.

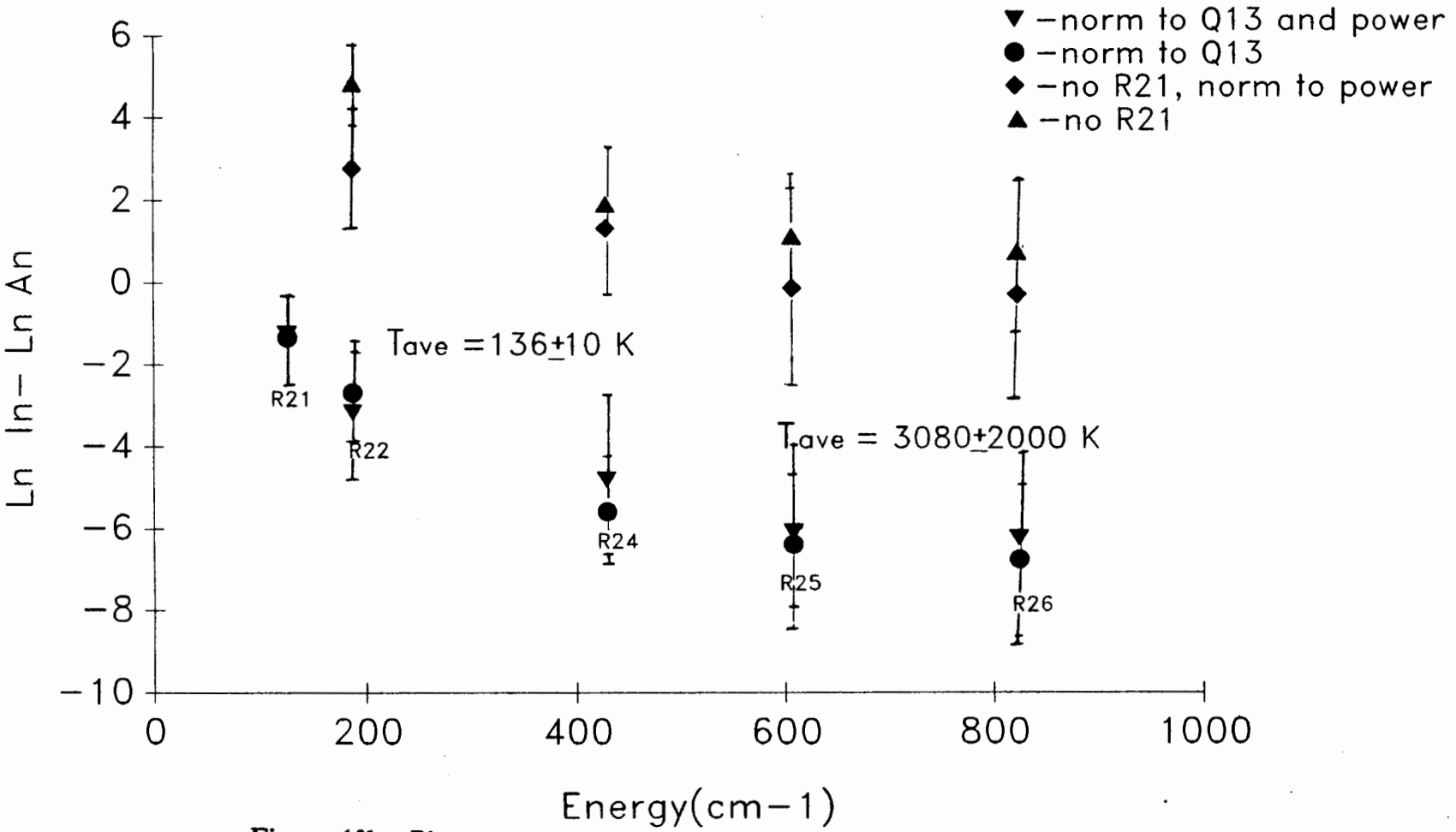

Figure 13b. Plot of intensity of HO from the ozone-water reaction versus energy. Same as figure 13, but using peak height to determine intensities.

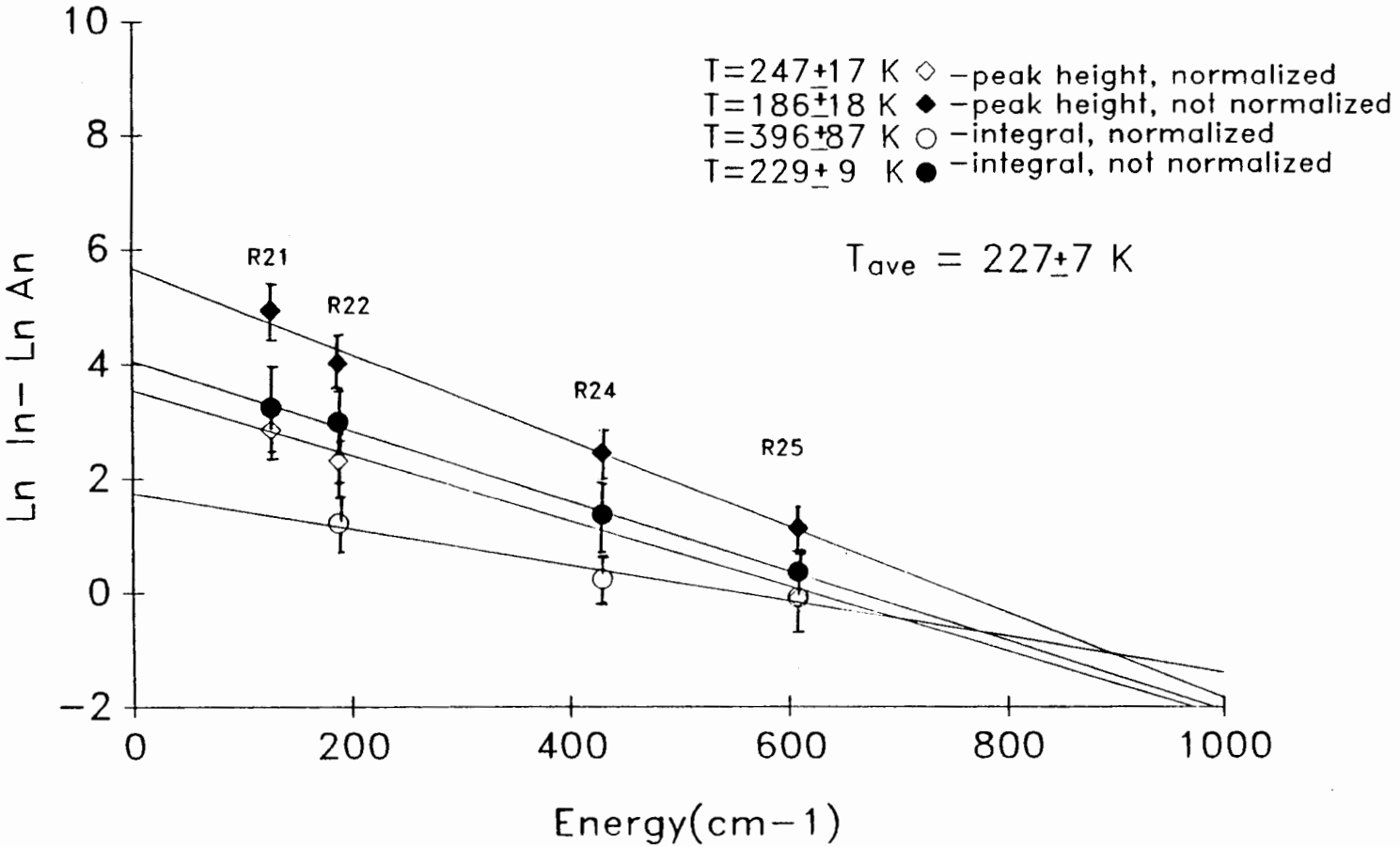

Figure 14. Plot of intensity of HO from the ozone-isobutane reaction versus energy. As in figures 12, 13a and 13b, the temperature was determined from the inverse of the slope.

TABLE XII

EXPERIMENTAL TEMPERATURE VALUES

RUN #	1	2	3	4	Ave.Temp.°K
HO:	375±58	291±9	423±32	420±31	310±8
^{1}O(D)-Isobutane:	186±18	247±17	229±9	396±87	227±7
^{1}O(D)-Water K = 1-4:	208±37	189±66	156±23	122±11	136±10
^{1}O(D)-Water K = 5-6:	7786	1639	2075	819	3080±2353

CHAPTER V

ERROR ANALYSIS

In this experiment as in all experiments we encountered two types of errors. The first type is present in every experiment with the same magnitude and the same sign and is due to uncertainties in calibration of the equipment and the way the technique is applied. They do not affect the precision of the results but affect their accuracy. These are systematic errors. The second type of errors appeared randomly through the data and vary from experiment to experiment, therefore have an effect on the precision of the results. These are random errors.

In this discussion the presence of systematic errors will be acknowledged but will not be treated in the analysis. Random errors in the other hand will be statistically analyzed.

SYSTEMATIC ERRORS

In this experiment there are two major sources of systematic errors. The first one is introduced by the rate of photon arrival on the photomultiplier tube.

If there is more than one photon arriving during one laser pulse there is the possibility that the second photon will not be detected and the recorded signal will be less than the real value. The second source of systematic error is the pulse discriminator used after the signal has been amplified and before it is actually counted. There is the possibility of missing pulses when their value lies under the discriminating level. It would be desirable to accurately calculate the absolute temperature but for our purposes only the relative values are important, therefore more emphasis will be set on the study of random errors.

RANDOM ERRORS

The error in the temperature determination depends on the uncertainties of the slope which in turn depends on the intensity, the counts and the power meter reading.

Laser Power

The error in the laser power was estimated to be $\pm$1mW, meaning that within one measurement the output varied as much as 1mW. This factor introduces the greatest source of error in the calculations given that the average observed power was about 3mW. A drift of 1mW in this value represents an error of about 33%. For this reason the plots of the non-normalized data were also studied.

Counts

The error in the counts was studied statistically using the Poisson distribution. The Poisson distribution is a special case of the binomial distribution in which the average number of successes is much smaller than the total possible number. For counting experiments where the data represents the number of items observed per unit of time there are always fluctuations. These arise not from a lack of precision in the measuring instrument, but from statistical fluctuations in the collection of a finite number of counts over finite intervals of time. If the same measurement could be done repeatedly we would find that the measurements spread out about the mean. The results can be modelled using the Poisson distribution and the error is defined to be:

$$\sigma_{counts} = counts^{1/2}$$

Intensity

The uncertainty in the intensity value whether normalized to power or not, was derived by propagating the error of the counts and the power meter through the appropriate equations. The general equation for error propagation for the intensity as a function of counts and laser power is:

$$^2(I) = (\partial I/\partial C)^2\sigma^2_c + (\partial I/\partial p.m.)^2\sigma^2_{p.m.} + 2\,(\partial I/\partial C)(\partial I/\partial p.m.)\sigma_c\sigma_{p.m.}$$

The counts and the laser power are assumed to be two independent quantities therefore the last term is equal to zero. The new equation is:

$$\sigma^2(I) = (\partial I/\partial c)^2\sigma^2_c + (\partial I/\partial p.m.)\sigma^2_{p.m.}$$

When this is solved for the appropriate relationship we get:

$$\sigma^2_{Intensity} = (Intensity)^2 (\sigma_c^2/c^2 + \sigma_{p.m.}^2/p.m.^2)$$

for the normalized cases. The fact that the plotted intensities are not just normalized to the laser power but also to the $Q_1 1$ line and the $Q_1 3$ line for the natural HO and the ozone-water HO respectively, was also taken in consideration and the error was propagated accordingly.

Slope

For the slope uncertainty and the slope itself, a least square algorithm which allowed weighting the data points was used. It was important to weight each point because the intensity values did not have the same uncertainty. In this procedure the error in the x variable is assumed to be zero, that is in our case, the energy values of the rotational levels are assumed to be accurate. The weight of each data point is calculated by:

$$W_i(total) = W_i(linearization) \times W_i(counts) \times W_i(power\ meter)$$

$$W_i(linearization) = (f')^{-2} = (\partial \ln I_i/\partial I_i)^2 = I^2$$

where I is the intensity and ln I is the natural log of the intensity

$$W_i(counts) = (\sigma_{i\ counts}^2)^{-1} = (counts_i)^{-1}$$

$$W_i(power\ meter) = \sigma_i^2 \approx 1$$

Temperature

The error in the temperature was calculated by propagating the error of the slope according to the equation:

$$T = [\text{slope} \times k]^{-1}$$

where k is Boltzmann constant.

From this the error is calculated to be:

$$\sigma_T = [(\text{slope}^2)^2 \sigma^2_{\text{slope}}]^{1/2} = (\sigma^2_{\text{slope}}/\text{slope}^4)^{1/2} = \sigma_{\text{slope}}/(\text{slope})^2$$

Average Temperature

The average temperatures were computed from the formula:

$$T_{\text{average}} = \frac{\sum W_1 T_1}{\sum W_1}$$

where $W_1 = \sigma_T^{-2}$

and the error for the average temperature value is:

$$\sigma_{\text{Tave}}^2 = (\Sigma W_i) \ , \ \sigma_{\text{Tave}} = (\Sigma W_i)^{1/2}$$

The obtained average values are:

natural HO:	310 ± 8 K
$O^1(D)$-isobutane HO:	227 ± 7 K
$O^1(D)$-water HO:	136 ± 10 K
	3080 ± 2353 K

CHAPTER VI

DISCUSSION

The purpose of this project was to evaluate the interference of photolytic HO on the measurements of atmospheric HO in the method of LIF-FAGE. Even though a definite percent of interference can't be obtained from the experimental data, some good qualitative observations can be made about the effectiveness and sensitivity of this method.

From an analysis of the results from the natural HO measurements, we conclude that the distribution of the population among its rotational levels follows a Boltzmann distribution. The obtained temperature measurement in the natural HO case, is actually the gas temperature. When this temperature is compared to the value obtained in the $O^1(D)$-isobutane case we can see that the natural HO temperature is higher. The difference between these temperatures can be explained in part by the fact that the natural HO was produced from the photolysis of water molecules induced by a mercury lamp which was situated directly over the FAGE nozzle inlet. This observation agrees with the results reported by Dr. Tom Hard, in a private communication where the temperature measured at the outflow from the mercury lamp was detected to be well above

room temperature. In previous studies done as precursors to this project, the temperature of the gas flow was measured at different positions inside the FAGE probe using a long, thin tube with a thermocouple at the tip, were done and a temperature drop of about 9° due to the pressure drop was observed. A drop from 299°K at room temperature, to 291°K inside the detection chamber was observed when the mercury lamp was not present (Figure 16 and Table XIII). Unfortunately, measurements with the mercury lamp in place were not done at the time. Nevertheless, this facts give support to the experimental results.

In the case of HO produced by the $O^1(D)$-isobutane reaction a thermal distribution is also observed for low values of K and the average temperature calculated is 227°K. This results present a potential problem in the FAGE method, since as it was stated before, this method depends on the reaction of isobutane with HO to calculate background noise. According to these results, the HO potentially produced by the reaction of isobutane with ozone, will cause interference with the detected signal. The specificity of this measurement method depends on the ratio of the HO produced by the isobutane reaction and the actual signal.

The lower temperatures observed in this case are explained in part by the absence of the mercury lamp over the nozzle (room temperature = 299°K, mercury lamp = 311°K : accounts for 12°K difference). The second reason for the colder temperature values might be related to the actual mechanism of the

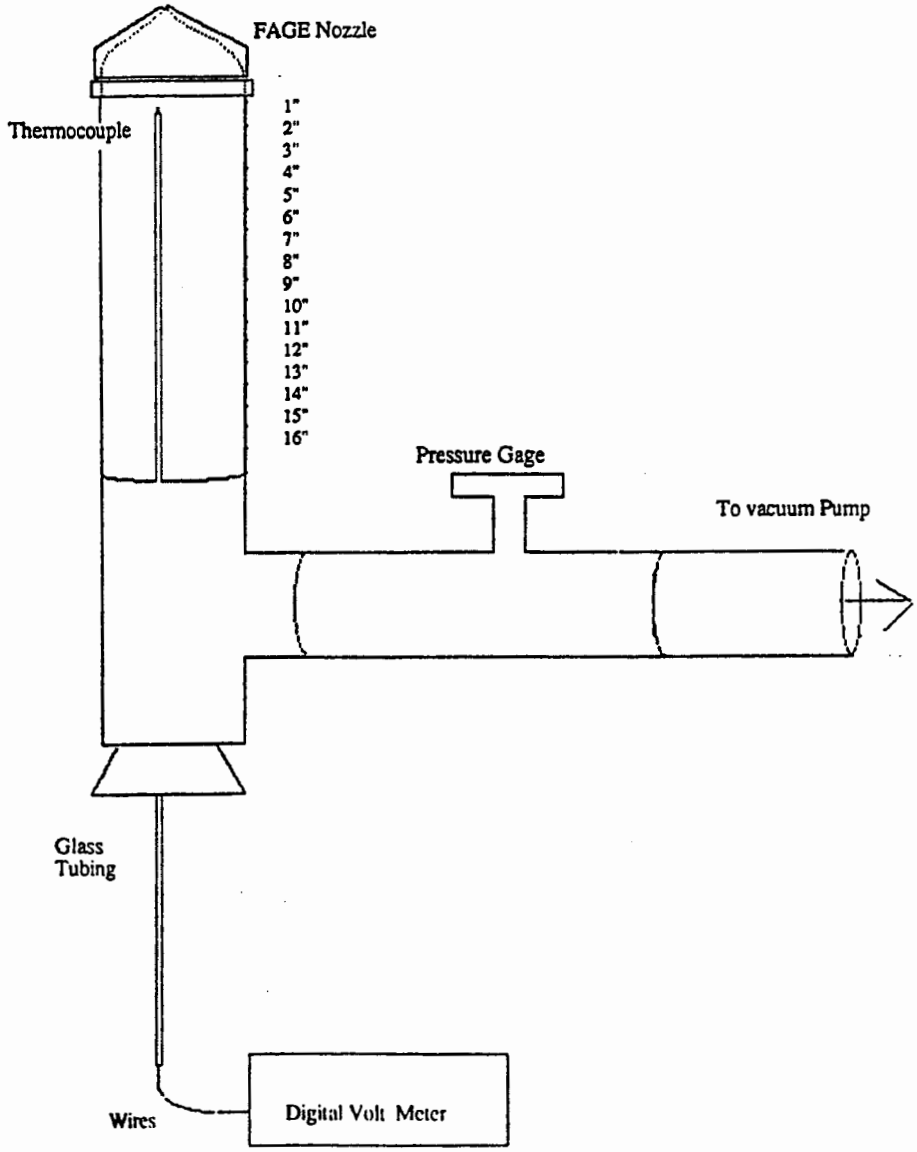

Figure 15. Experimental setup for direct temperature determination in the thermocouple experiment.

TABLE XIII

DIRECT TEMPERATURE MEASUREMENTS INSIDE FAGE PROBE USING A THERMOCOUPLE

ROOM TEMPERATURE: 299°K

DISTANCE FROM NOZZLE	TEMPERATURE
≈0"	291.60
3"	291.58
4"	292.58
5"	292.75
6"	292.89
7"	292.18
8"	292.03
9"	292.04
10"	292.50
11"	292.07
12"	291.75
13"	291.58
14"	291.53
15"	291.28

TABLE XIII

DIRECT TEMPERATURE MEASUREMENTS INSIDE FAGE PROBE USING A THERMOCOUPLE
(continued)

DISTANCE FROM NOZZLE	TEMPERATURE
17"	292.07
18"	291.94
19"	291.51
20"	291.56
21"	291.67
22"	291.16
23"	291.64
24"	291.03
25"	291.00
26"	290.67
27"	290.46
28"	290.40
29"	290.20
30"	290.76

reaction. According to a study by Luntz (1980) where the mechanism for the HO formation from several saturated hydrocarbons and $O^1(D)$ was studied, the reaction can occur by two different pathways: insertion and abstraction. The insertion method is dominant in small molecules while the abstraction methods is favored as the number of carbon atoms in the molecule increases. In the insertion method the theory indicates the formation of a "hot" intermediate while in abstraction there is no formation of a "hot" intermediate, therefore a rotational "hot" HO is not expected. This is the case for isobutane. For the $O^1(D)$-water case two distinct rotational distributions were observed, one for the lower values of K (K = 1 to 4), and the second one for higher values of K (K = 5 to 6). This indicates that the population distribution among this molecule's rotational levels is not statistical, the molecule is energetically "hot". In general terms it means that this molecule does not have the same spectroscopic characteristics as the natural HO, therefore not all the molecules will interfere with the measurement of the radical. Similar results were also reported by Rodgers et. al. (1981) and Gericke et. al. (1980). These researchers report temperatures of 500°K and 400°K for K = 1 to 6, and temperatures of 2500°K and 1900°K for K = 7 to 15 respectively. They calculated that half of the molecules will have a statistical population due to the mechanism of the reaction and that by the time of detection about 25% of the "hot" molecules will be relaxed into a statistical distribution.

The observed divergence from a the first statistical distribution in this

project, was observed at K = 5. This seems to indicate that at the moment of detection, less molecules were thermally distributed among the rotational levels than in Rodger's and Gericke's report. Even though a detailed quantitative analysis of the photolytic interference in FAGE can't be done at this time due to lack of data on larger values of K, from the results it can be inferred that the level of interference in the FAGE method is less than the one reported for LIF experiments at atmospheric pressure.

There are three major factors contributing to the reduction of interference in the LIF-FAGE method. First, the lower pressure with its consequent gas expansion reduces the total amount of molecules present for excitation (includes HO and ozone), but at the same time it reduces the quenching of the HO molecules due to collisions so there is an increase in the fluorescence lifetime. Second, the lower energy per pulse provided by our new copper vapor-dye laser system, reduces the production of photolytic species and it further decreases the resulting signal (since this one varies with the square of the laser power). The last factor which contributes to the lowering of the photolytic interference, is our highly sensitive electronic detection system which allows us to detect a true nascent distribution. As the experimental pressure value decreases, the chances of collisional quenching also decreases and the fluorescence lifetime will be longer. If a lower pressure is accompanied with a short delay time, or a narrow laser pulse, less molecules will be relaxed to an equilibrium distribution at the time of detection. A parameter that can be used in order to compare

the efficiency of detecting a true nascent population is the product $P\Delta t$, where P is the experimental pressure and Δt, is the time delay between two laser pulses or in our case where only one laser was used, Δt is approximately the laser pulse width. Unfortunately, the reports of Gericke and Rodgers do not give enough information to compare this parameter. The lowest possible value of this product is desired. For this experiment the product $P\Delta t$, is 68 Torr ns.

REFERENCES

Anderson, J.G., Geophys.Res.Lett., 3, No.3, 165 (1976).

E.L. Baardsen, and R.W. Terhune, App.Phys.Lett., 21, No.5, 209 (1972).

C.R. Burnett, Geophys.Res.Lett., 3, No.6, 319 (1976).

M.J. Campbell, J.C. Sheppard, and B.F. Au Geophys.Res.Lett., 6, No.3, 175 (1979).

C.D. Carter, J.T. Salmon, G.B. King and N.M. Laurendeau, Appl.Optics, 26, No.21, 4551 (1987).

W. Chameides and J.C.G. Walker J.Geophys.Res., 78, No.36, 8751 (1973).

C.Y. Chan, Portland State University, Ph.D. Thesis 1982.

C.Y. Chan, R.J. O'Brien II, T.M. Hard, and T.B. Cook, J.Phys.Chem., 87, 4966 (1983).

P.J. Crutzen and J. Fishman, Geophys.Res.Lett., 4, No.8, 321 (1977).

D.D. Davis, W. Heaps, and T. McGee, Geophys.Res.Lett., 3, No.6, 331 (1976).

D.D. Davis, W.S. Heaps, D. Philen, M. Rodgers, T. McGee, A. Nelson, and A.J. Moriarty, Rev.Sci.Instrum. 50, No.12, 1505 (1979).

D.D. Davis, M.O. Rodgers, S.D. Fischer and K. Asai, Geophys. Res.Lett., 8, No.1, 69 (1981).

D.D. Davis, S.D. Fischer and M.O. Rodgers, Geophys.Res. Lett., 9, No.1, 101 (1982).

G.H. Dieke and H.M. Crosswhite, J.Quant.Spectrosc.Radiat.Transfer, 2, 99 (1961).

K.H. Gericke and F.J. Comes, Chem.Phys.Lett., 74, No.1, 63 (1980).

T.M. Hard, C.Y. Chan, A.A. Mehrabzadeh, W.H. Pan, and R.J. O'Brien, Nature, 332, 617 (1986).

T.M. Hard, R.J. O'Brien, C.Y. Chan and A.A. Mehrabzadeh, Environ.Sci. Technol., 18, 768 (1984).

W.S. Heaps and T.J. McGee, J.Geophys.Res., 90, No.D5, 7913 (1985).

W.S. Heaps and T.J. McGee, J.Geophys.Res., 88, No.C9, 5281 (1983).

C.N. Hewitt and R.M. Harrison, Atm.Environ., 19, 564 (1985).

H.P. Hooymayers and C.Th.J. Alkemade,J.Quant.Spectros. Radiat.Transfer, 7, 495 (1967).

D.K. Killinger and C.C. Wang, Chem.Phys.Lett., 52, No.2, 374 (1977).

D.K. Killinger and C.C. Wang, J.Chem.Phys., 71, No.4, 1582 (1979).

H. Levy II, Science, 173, 141 (1971).

J.A. Logan, M.J. Prather, S.C. Wofsy, and M.B. McElroy, J.Geophys.Res. 86, No.C8, 7210 (1981).

A.C. Luntz, J.Chem.Phys, 73, No.3, 143 (1980).

M. Manabusa and C.C. Wang, J.Chem.Phys., 66, No.5, 2118 (1977).

I.S. McDermid, J.B. Laudenslager and T.J. Pacala, Appl. Optics, 22, No.17, 2586 (1983).

H. Mohan and Shardanand, "Free Radical OH", Scientific and Technical Information Office, NASA, Washington D.C. (1975).

R.G. Mortimer, MacMillan Publishing Co., Inc., (1981) Chpt. 10.

R.J. O'Brien and B.E. Dumdei, Anal.Chem., 56, No.8, 1329 (1984).

R.J. O'Brien, T.M. Hard and A.A. Mehrabzadeh, Environ.Sci. Technol., 17, 562 (1983).

D. Perner, D.H. Ehhalt, H.W. Patz, V. Platt, E.P. Roth and A. Volz, Geophys.Res.Lett., 3, No.8, 466 (1976).

D. Perner, D.H. Ehhalt, H.W. Patz, U. Platt, E.P. Roth, and A. Volz, Geophys.Res.Lett., 3, No.8, 466 (1976).

M.O. Rodgers, K. Asai and D.D. Davis, Chem.Phys.Lett., 78, No.2, 246 (1981).

P.M. Selzer and C.C. Wang, J.Chem.Phys., 71, No.9, 3786 (1979).

D.D. Shoemaker, C.W. Garland, J.I. Steinfield and J.W. Nibler, McGraw Hill, Inc., (1981), Chpt. 2 and Chpt.10.

F.P. Tully, Chem.Phys.Lett., 96, No.2, 148 (1983).

C.C. Wang, L.I. Davis, Jr., C.H. Wu and S. Japar, Appl.Phys. Lett., 28, No.1,14 (1976).

C.C. Wang and L.I. Davis, Jr., Appl.Phys.Lett., 25, No.1, 34 (1974).

C.C. Wang and L.I. Davis, Jr., Geophys.Res.Lett., 9, No.1, 98 (1982).

C.C. Wang, L.I. Davis, Jr., and P.M. Selzer, J.Geophys.Res. 86, No.C2, 1181 (1981).